Different morphologies of MnO_2 nanostructures for the photocatalytic oxidation and photoreduction

Thesis submitted in the partial fulfillment of the

requirement of the degree of

MASTERS OF SCIENCE

IN

CHEMISTRY

Submitted By

Devanshi Tinna

Roll no: 301502012

UNDER THE SUPERVISION OF

Dr. Bonamali Pal

Professor

School of Chemistry and Biochemistry,

Thapar University, Patiala-147004

Punjab (India)

July, 2017

Certificate

This is to certify that the thesis entitled **"Different morphologies of MnO_2 nanostructures for the photocatalytic oxidation and photoreduction"** being submitted by **Ms. Devanshi Tinna** in partial fulfillment of the requirements for the award of degree of Master of Science in Chemistry to the School of Chemistry and Biochemistry, Thapar University, Patiala, is a bonafide work carried out by her under my supervision. The contents of this thesis have not been submitted for the award of any other degree or diploma.

Dr. Bonamali Pal
Professor,
School of Chemistry and Biochemistry,
Thapar University, Patiala - 147004

Candidate's Declaration

I hereby declare that the work being presented in the thesis entitled **"Different morphologies of MnO_2 nanostructures for the photocatalytic oxidation and photoreduction"** in partial fulfillment of the requirements for the award of degree of Master of Science in Chemistry, and being submitted to School of Chemistry & Biochemistry, Thapar University, Patiala, is my own work during the period of January to July 2017, under the supervision of Dr. Bonamali Pal. I have not submitted the contents embodied in this thesis for the award of any other degree.

Date:

Devanshi

(Devanshi Tinna)

Place: Patiala

This is to certify the above statement made by Ms. Devanshi Tinna is correct and true to the best of my knowledge.

Dr. Bonamali Pal
Professor,
School of Chemistry and Biochemistry,
Thapar University, Patiala - 147004

ACKNOWLEDGEMENTS

I am thankful to my supervisor **Dr. Bonamali Pal**, Professor School of Chemistry and Biochemistry, Thapar University, Patiala for his keen interest, expert guidance, and motivation during my thesis.

A special thanks for helpful and encouraging attitude of **Dr. Amjad Ali,** Associate Professor and Head, School of Chemistry and Biochemistry, Thapar University, Patiala for providing necessary facilities.

I am very grateful to my mentor **Mr. Rayees A. Rather** for his guidance, support, encouragement and suggestions throughout the period. I extend my special thanks to the PhD Scholars **Ms. Sakshi Bhardwaj, Mrs. Ritika Julaha, Ms. Manpreet Kaur Aulakh, Mr. Aadil Bathla, Ms. Tanushre Basu, Mrs. Samriti Thakur** and **Mr. Roop Chand Prajapat** for their immense cooperation, timely help and moral support provided by them during the complete span of my project.

I would also like to acknowledge my labmates and other faculty members for their cooperation during my work. I owe special thanks to my parents for their moral support throughout my life.

Place: Patiala Devanshi Tinna

List of contents

List of abbreviations

NPs	Nanoparticles
UV	Ultraviolet
Vis	Visible
DRS	Diffuse Reflectance Spectrophotometer
EDX	Energy Dispersive X-Ray
SEM	Scanning Electron Microscopy
%	Percentage
a.u	Arbitrary Unit
Nm	Nanometer
μL	Microliter
Ppm	Parts Per Million
˚C	Degree Celsius
Mg	Milligram
MnO_2	Manganese Dioxide (iv)
DLS	Dynamic Light Scattering
mM	Millimolar
eV	Electronvolt
mAU	milli Absorption Unit
MB	Methylene Blue
Mm	millimeter
Hg	Mercury

Abstract

This study shows photocatalytic activity of various morphologies of MnO_2 nanomaterial prepared via different hydrothermal methods for the photo oxidative decomposition of toxic methylene blue (0.01mM) under solar irradiation and photo reduction of nitrobenzene (25μM) to aniline again under solar irradiation. The resulting materials were characterized by XRD, SEM, EDS, DRS, DLS and fluorescence spectroscopy. MnO_2 is a promising photocatalyst for photo oxidation and photoreduction due to its low cost, high stability and low toxicity. Moreover, different shapes exhibit different catalytic activities. Alpha MnO_2 nanotubes and beta MnO_2 nanorods gives better activity in photo oxidation while alpha nanotubes alone gives better activity in photo reduction. This enhancement in photocatalytic activity is due to different shapes of MnO_2 which enlarges its surface area for the reaction. The photo oxidation reaction follows pseudo first order kinetics. GC analysis showed the complete photomineralization of methylene blue to CO_2 and H_2O.

Keywords: Methylene Blue degradation, Alpha MnO_2 nanorods, Alpha MnO_2 nanowires, Beta MnO_2 nanorods, Gama MnO_2 nanosheets, MnO_2 Nanospheres, Alpha MnO_2 nanotubes, Nitrobenzene reduction

Introduction

In recent years nanotechnology is emerging vastly in field of research and technology. Nanotechnology deals with nanostructures of small size with dimensions ranging from sub nanometers to several nanometers. Nanostructures with different structure and sizes have shown as effective catalysts [1]. Nanostructures have been used for catalysis because of their various structures with high surface area to volume ratio [2].

Catalysts are the workhorses of chemical changes. Catalysts fastens the chemical reaction by forming the chemical bonds with the reacting molecules [3], by allowing these to react with the products and disconnect its bond with the catalyst and leaves it unchanged so it is available for the next reaction. A catalytic reaction may also be represented as a cyclic activity in which catalyst itself participates and is recovered into its original form at the end of the cyclic activity. The idea of catalysis was given by Elizabeth Fulhame and was later used by Jons Jokob Berzel us in 1835 to explain certain reactions that are increased by the use of substances that remain unaltered after the reaction [4].

Modern technology of catalysis is of great significance as it affects our daily life. Several major sections of the world's economy: petroleum and energy production, chemicals and polymer production, food industry and pollution control, involve catalytic processes [5].

Catalysts are used for formation of fuels (such as gasoline, diesel, heating oil, fuel oil), plastics, synthetic rubbers, fabrics, cosmetics, clean energy from renewable energy sources (such as hydrogen for fuel cells and transportation fuels from non-edible biomass). By using catalysts the use of toxic and hazardous reagents can be avoided and the use of undesirable products can be minimized. Catalysis is echo-friendly and is one of the most valuable principles out of twelve principles of Green Chemistry [6]

Catalytic processes can be divided into two major categories

a. **Homogeneous catalysis:** In homogeneous catalysis, the catalyst is in the same phase as the reactants i.e. here the reactants and catalysts are in one single liquid phase or in gas

phase. Very often industrial homogeneous catalytic processes are carried out in liquid phase [7]. Ester hydrolysis including general acid-base catalysts, polyethylene production with organometallic catalysts and enzyme catalyzed processes are few important instances of industrial homogeneous catalytic processes.

b. **Heterogeneous catalysis:** In heterogeneous catalysis, the catalyst and the reactant are in different phases, the most common example includes formation of sulfur dioxide by contact process [8]

Heterogeneous catalysts are basically "supported," which indicates that the catalyst is dispersed on the other side heterogeneous catalyst is a material that fastens the effectiveness or decreases their cost. Generally, the heterogeneous catalysts are solids which act on substrate surface in a liquid or gaseous reaction mixture. Several mechanisms for these reactions on surfaces are popularly known, regulated by how the adsorption arise. The minor the catalyst particle size, the major the surface area for the given mass of particles.

In heterogeneous catalysis, the reactants diffuse to the surface of catalyst and adsorb onto it, by forming new chemical bonds. After the reaction, product molecules desorb from the surface and diffuse apart. The transport process and surface chemistry like dispersion is of great importance [9].

The term "Photocatalyst" itself defines its meaning i.e. "light acting as catalyst". Simply, acceleration of photoreaction due to presence of catalyst [10]. Chlorophyll of plants is essential photocatalyst. Here, the plant captures the energy from sunlight and grows, producing oxygen. The difference between chlorophyll (natural) photocatalyst and artificial photocatalyst is that chlorophyll catches the sunlight to turn water and CO_2 into O_2 and glucose, but the other photocatalyst produces strong oxidizing agent and electronic holes to tear the organic molecules to CO_2 and water in presence of photocatalyst, light and water

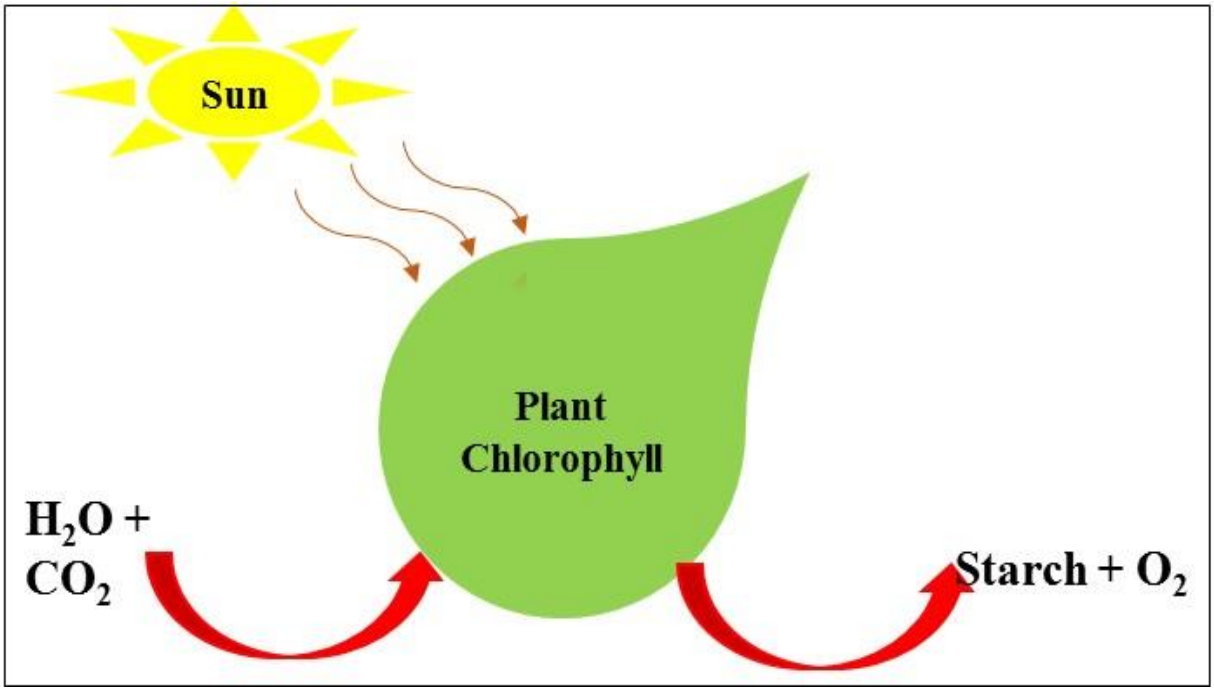

Scheme 1: Mechanism of chlorophyll as natural photocatalyst

Photocatalytic activities focuses the number of research activities and particular effect is given on reduction of organic compounds and degradation of many dyes.

Before knowing about the mechanism of photocatalysis we need to know about energy of electrons in insulator, conductor and semiconductor. The fermi level is defined as surface of that sea at absolute zero where no electrons will have enough energy to rise above the surface.

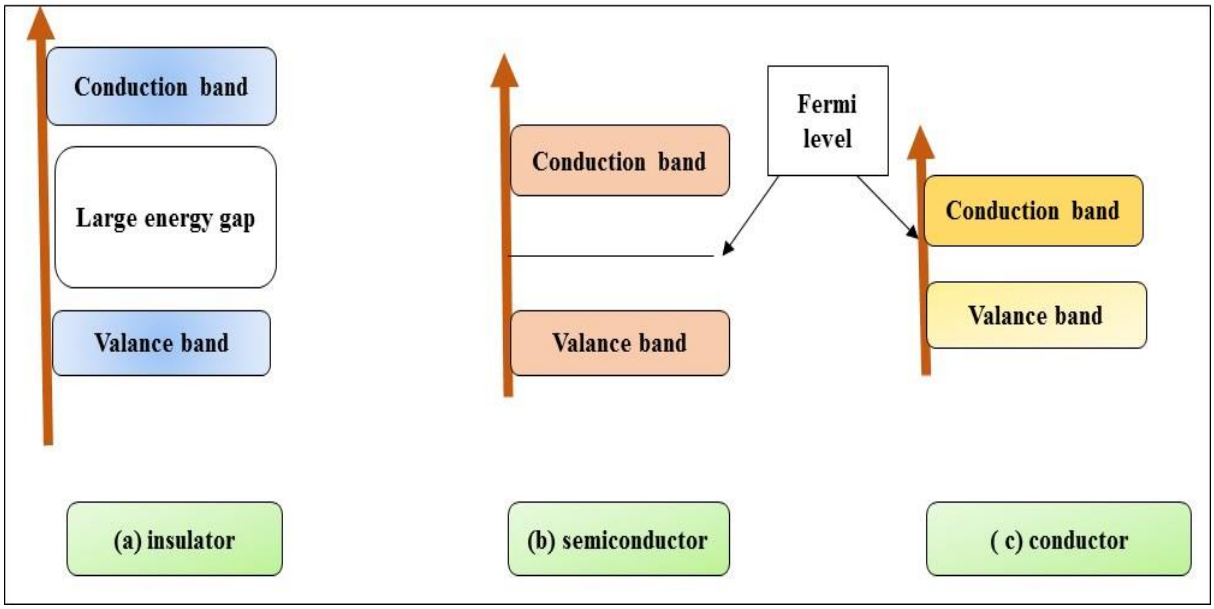

Scheme 2: Energy of electrons in insulator, conductor and semiconductor

The energy of a semiconductor's band gap is equal to the difference in energy between the conduction band edge and the valence band edge. Band edge energy levels are most commonly used photo catalysts.

Table 1: Band gaps of various catalysts.

Nanoparticles	**Band gap (eV)**
TiO_2	**3.2-3.0**
MnO_2	**2.92**
WO_3	**2.8**
CdS	**2.5**
ZnS	**3.6**
ZnO	**3.2**

Mechanism of photo catalyst includes:

1. Photocatalyst first absorbs light from the source.
2. Electron present in valance band gets excited to the conduction band.
3. Thus in valance band, formation of positive holes take place.
4. Energy gap between valance band and conduction band is known as band gap.

5. Reduction takes place in conduction band due to presence of free electrons.
6. Oxidation takes place at valence band.

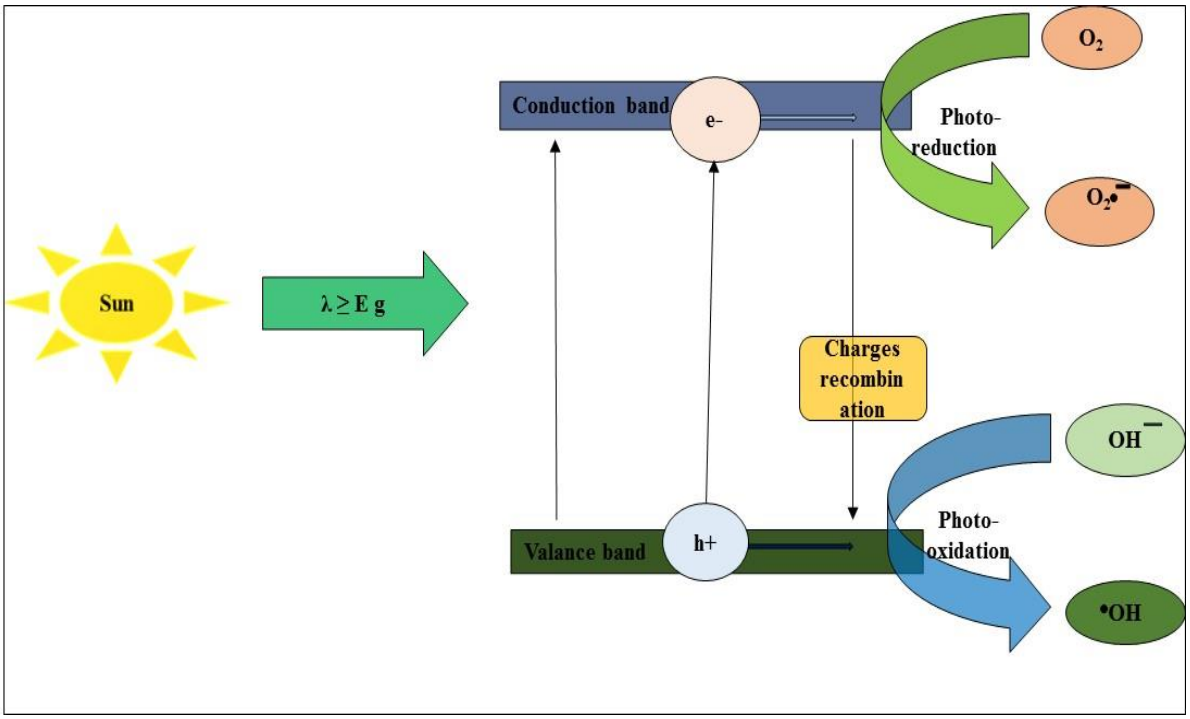

Scheme 3: Mechanism of photocatalysis

First period of transition metals are depicted by these metals.

Sc Ti V Cr Mn Fe Co Ni Cu and Zn

These accommodate the presences of *d* electrons (partly filled or unfilled *d* orbitals). Thus these transition metals form compounds of changeable oxidation states. The absorption strength also alters with the metals. Generally, the absorption is the strongest for metals on the left, and it decreases for transition metals in a period as the atomic number increases. When oxygen atom binds to transition metal atom it forms transition metal oxides. For photocatalysis, transition metal oxides are chosen as liable photocatalysts.

MnO_2 as photo catalyst

With the rigorous environmental issues toxic metal ions are the major contaminants. These compounds are very toxic to all forms of life and can be detected in major concentration in industrial waste water. One possible way to reduce the concentration of these compounds is the use of heterogeneous catalyst due to low chemical addition, attainability and low price for industrial processes. MnO_2 is the most employed photocatalyst due to its favorable

photochemical properties. Manganese (IV) oxide catalyst generally speeds up the decomposition of hydrogen peroxide (H_2O_2) to water and oxygen gas.

In recent years, we have been involved in an unfolding story whose main character is an interesting material MnO_2 (Manganese dioxide). The story began with the charge storage mechanism of MnO_2 electrode used in aqueous electrochemical capacitor [11] and then started to shift into the areas of environmental photocatalysis.

The 2-D structure of MnO_2 is

Fig 1. 2-D structure of MnO_2

The 3-D structure of MnO_2 is a rutile structure shown in Fig 2. where oxygen atoms are red coloured and metal atoms are grey coloured.

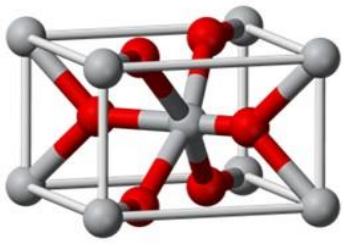

Fig 2. 3-D structure of MnO_2

There are various forms mineral polymorphs of MnO_2.

A. Pyrolusite (β-MnO_2), contains individual chains of edge-sharing Mn (IV) O (VI) octahedra and share corners with the side by chains to form a network like structure containing gaps with square areas that are one octahedron by one octahedron on a side.

B. Ramsdellite- rare mineral, generally present in low-temperature hydrothermal deposits.

C. Nsutite (γ-MnO_2), a vital cathodic material utilized for dry-cell batteries.

Properties of MnO_2

Manganese (IV) oxide is the inorganic compound with high adsorption capacity and adsorption kinetics. Some properties of manganese dioxide:

Table 2: Properties of MnO_2

1.	**Colour**	**Dark Brown**
2.	**Molar mass**	**86.93 g/mole**
3.	**Density**	**5.026 g/cm^3**
4.	**Melting point**	**535 °C**
5.	**Solubility in water**	**Insoluble**
6.	**Appearance**	**Black-brown solid**
7.	**Crystal structure**	**Tetragonal**
8.	**Point group**	**D_{4h}**
9.	**Magnetic property**	**Ferromagnetic**
10.	**Melting Point**	**535 ^{0}C**

Applications

MnO_2 is reactant that was first used on positive side of very common alkaline cells that have zinc as negative electrode material. Recently MnO_2 is used in batteries which is produced electrolytically and is termed as Electrolytic Manganese Dioxide (EMD). The major applications includes:

1. Electrochemical Catalysis of Styrene Epoxidation [12].
2. Interface for remarkably promoting catalytic oxidation activity
3. Liquid phase aerobic oxidation of benzyl alcohol [13].
4. Photodegradation of dyes
5. Degradation of various toxic chemicals
6. As superior catalyst for Nitro compound reduction

Literature review

People began forming new electrode material for electrochemical capacitor, consisting of metal oxide, since 1970s. Because of promising power and energy, MnO_2 has been found capable for application of supercapacitor. More significantly, green nature and natural abundance of MnO_2 [14], will lower the cost compared to noble metal oxides.

Basically, utility of MnO_2 is related to degradation of dyes, reduction of nitro compounds and production of batteries, such as the alkaline battery and the zinc-carbon battery [15]. Moreover, MnO_2 is also a precursor to produce other manganese compounds, such as $KMnO_4$ or $MnSO_4$. Impurities are contained in natural manganese oxide. Hence, synthetic manganese oxide production is important. Synthetically manganese oxide is produced by two major methods, EMD (Electrolytic manganese oxide) and CMD (Chemical manganese oxide). During production of batteries, EMD is used while producing ferrites CMD is used [16]. Various complex oxides of manganese exists such as MnO_2, Mn_2O_3 and Mn_2O_7 because of variable oxidation state of manganese (+3, +4, +5 and +7). Manganese oxide materials have extreme importance in technological applications such as: supercapacitor, photo catalysis, cathodic materials in Li batteries. [17-18] and ion sieves etc. Largest number of polymorph structures is exhibited by MnO_2 among all oxides of manganese. It has small ionic radius of Mn^{4+} (R = 0.53 Å) which may result in tetrahedral coordination. Octahedral coordination is stabilized by $3d^3$ electronic configuration of Mn^{4+}. In oxides, that leads to the absence of tetrahedral coordinated Mn^{4+} [19-20].

Simply in all MnO_2 structures, $Mn^{4+}$is present in the interstices of various close-packed networks of oxygen atoms [21]. This complication is the reason for which various types of cation ordering schemes are manageable in MnO_2.

Juqin Zeng and his co-workers synthesized alpha MnO_2 Nanorods through reduction of $KMnO_4$ in acidic solution that shows high specific surface area of $156 m^2 g^{-1}$.It has high recharge efficiency (~ 90%) and retention capacity. α- MnO_2 catalyst combined with ionic liquid based electrolyte is an effective combination to improve capacity and durability of rechargeable lithium- O_2 batteries [22]. Debart Aurilie et.al. Synthesized alpha MnO_2 nanowires depicted that it has high charge capacity and hence used for oxygen electrode in rechargeable Lithium batteries [23]. Yongtao Meng et al. synthesized different structures of Manganese oxides (α-, β-,

and δ- MnO_2) by various facile methods, where MnO_2 Nanoparticles reveals electro catalytic features [24]. Min-Sik Park et al. prepared alpha MnO_2 nanowires and nanopowders to promote the comparison of their catalytic activity in application of Li- air batteries [25].

Naveen Mittal and his co-workers performed their work on photocatalytic degradation of Rose Bengal dye in presence of sunlight with MnO_2 nanoparticles. At λ_{max} 559 nm photocatalytic bleaching of RB was observed [26]. Jiantuan Ge et al. investigated the degradation of azo dye acid red B (ARB) with MnO_2 in the absence/presence of ultrasonic irradiation (sonication). Results showed that decolorization is much huge in presence of ultrasonic irradiation compared to using MnO_2 alone [27]. Li Shunjun et al. studied the influence of MnO_2 nanomaterials on photocatalytic activity of P-25TiO_2 in degradation of methyl orange dye. Sometimes, due to presence of a little amount of MnO_2 nanoparticles in TiO_2 particles, the photocatalytic activity of TiO_2 may be inhibited or even completely destroyed [28]. Shunjun Li et al. also studied the causes of presence of various MnO_2 nanoparticles alpha- MnO_2, beta- MnO_2 and gama- MnO_2 on degradation of phenol. The results revealed that the TiO_2 photocatalytic degradation of phenol was poisoned completely in start of 20–60 min during the presence of MnO_2 while ZnO photo catalytic degradation of phenol only declined slightly [29].

Weixin Zhang and his coworkers synthesized (ß-MnO_2) nanorods hydrothermally by thermal decomposition of MnOOH, and by using $KMnO_4$ in an aqueous ethanol solution. The comparison of catalytic efficiency of MnO_2 nanopowder and nanorods demonstrated that catalytic efficiency of ß-MnO_2 nanorods for oxidation of methylene blue dye in the presence of H_2O_2 is higher than Micro sized ß-MnO_2 nanopowder [30].

Subhra Jana et al. synthesized the photo catalyst, superparamagnetic monodispersed spherical beta-MnO_2 of size~10 nm and band gap ~ 2.52 eV have been prepared in toluene which help the oxidative phenol coupling reaction [31]. Mohammad Mahdi Najafpour et al. synthesized Mn Oxides and showed their catalytical support for water oxidation in presence of Ce [32]. Alcohol oxidizing activity of manganese were reported. Manganese oxide catalysts were considered liable catalysts for oxidizing some alcohol to aldehydes in presence of ozone [33].

Naturally Mn oxides are used to control heavy metal amounts in soil and in aquatic sediments [34, 35] then nano layered Mn Oxides were synthesized and Ag was deposited on it. Catalytic results revealed that the irradiated systems rapidly cause phenol degradation [46].

Research Gap

The above literature showed about various applications of MnO_2 nanoparticles in rechargeable batteries production, photo-reduction and various studies about photo-oxidation. However it also suffer from few drawbacks such as slow reduction of nitro compounds and slow oxidation of some dyes or sometimes changing one reactant to product may produce some toxic intermediates. Therefore there is need of improving the photocatalytic activity of MnO_2 for photo-reduction and photo-oxidation. This can be achieved by synthesizing these MnO_2 nanoparticles at various calcination temperatures which may form various shapes of MnO_2 nanoparticles with improved photocatalytic activities. Thus comparative study can be done from which we can estimate the activities of the photocatalyst.

Moreover little information is available about photo reduction of toxic nitro compounds and photo oxidation of methylene blue dye using various shapes of MnO_2 photocatalyst.

Objectives

1. Synthesis of anisotropic nanostructures of MnO_2 by various methods.
2. To study surface structure and photocatalytic properties of various morphologies of MnO_2 under sunlight and characterize these morphologies of MnO_2 nanoparticles by various techniques such as: SEM, XRD, DRS etc.
3. To study oxidation of methylene blue dye and reduction of nitrobenzene with as synthesized MnO_2 nanomaterial.

Experimental section

The experimental section contains chemicals and reagents used during research work which include chemicals, some instruments like magnetic stirrer, weighing balance, sonicator, muffle furnace, labortary centrifuge, hot air oven, UV-Visible spectrophotometer, GC, HPLC etc, different glassware and various techniques for characterization of photocatalyst.

Reagents and Chemicals

$KMnO_4$, $MnSO_4.H_2O$, SDBS, $MnCl_2$, urea, polyethylene glycol were used in preparation of MnO_2 morphologies and purchased from Loba chemicals. Hydrochloric acid with specific gravity of 1.0 g/ml and molecular weight of 36.458 g/mol was purchased from Loba Chemicals. The solvents Ethanol (C_2H_5OH), methanol (CH_3OH) and isopropyl alcohol ($CH_3CHOHCH_3$) of molecular masses 46.07 g mol^{-1}, 32.04 g mol^{-1}, and 120.192 g mol^{-1}respectively were used. Distilled water was obtained from millipore system. Argon gas was purged into test tubes for creating inert atmosphere.

Methodology

We preferred hydrothermal method to prepare different morphologies of manganese oxides.

Alpha MnO_2 nanowires

Alpha nanowires were synthesized by initially taking 0.478g of $KMnO_4$ and 0.51 g of $MnSO_4.H_2O$ and mixed together to form a homogeneous reaction mixture of 30 mL in aqueous solution. Then this mixture was transferred to autoclave and temperature of 140°C was maintained for 24 hours. Then the product was filtered, washed with milli-Q distilled water and ethanol (or dysol) and dried in oven at 60°C for two days [45].

Alpha MnO_2 nanorods

Alpha MnO_2 nanorods were synthesized by mixing 0.39g of $KMnO_4$ with 0.172g of $MnSO_4.H_2O$ for making 35 ml homogeneous aqueous solution. This mixture was then transferred to teflon lined stainless steel autoclave at 180°C for 16 hours. The product was filtered, washed with milli-Q distilled water and ethanol (or dysol) and dried in oven at 60°C for two days [45].

Alpha MnO_2 nanotubes

0.452g of $KMnO_4$ was added to 1 ml of 37% HCl to make 40ml mixture which was treated hydrothermally at 140°C for 12 hours. The product was filtered, washed with milli-Q distilled water and ethanol (or dysol) and dried in oven at 60°C for two days [45].

Beta MnO_2 nanorods

For synthesis of beta MnO_2 nanorods, 0.20g $KMNO_4$ and 4.0 ml of polyethylene glycol (400) were mixed with 80 ml deionized water and kept under rapid magnetic agitation at room temperature for 10 minutes. This mixture was transferred to autoclave at 160°C for 5 hours. The product was filtered, washed with milli-Q distilled water and ethanol (or dysol) and dried in oven at 60°C for two days [41].

Gama MnO_2 nanosheets

For synthesis of gama MnO_2 nanosheets, 1.3g SDBS and .40g $MnCl_2.4H_2O$ were mixed to 4.5 ml deionized water and kept under rapid magnetic agitation at room temperature for 30 minutes. This mixture was then transferred to autoclave at 110°C for 12 hours. The product was filtered, washed with milli-Q distilled water and ethanol (or dysol) and dried in oven at 60°C for two days [41].

MnO_2 nanospheres

These were synthesized by mixing 0.005mol $KMnO_4$ with 40 ml distilled water followed by magnetic stirring for 20 minutes. During the stirring, 10 ml of 6M HCl was added dropwise to the mixture and then further stirring was continued for 4 hours. After proper stirring, the mixture was centrifuged for 10 minutes. Again washing was given for 2-3 times during centrifugation [50].

Photocatalytic activity

Photocatalytic degradation of methylene blue dye

Methylene Blue also known as Swiss Blue or Methylthioninium Chloride, having chemical formula $C_{16}H_{18}ClN_3S$ was purchased from Loba Chemicals has been prominantly used for drug indications. It has molecular weight of 319.851 g/mol. Soluble in ethanol, chloroform with vapour pressure $1.30X10^{-7}$ mm Hg at 25°C and melting point 100 to 110°C.

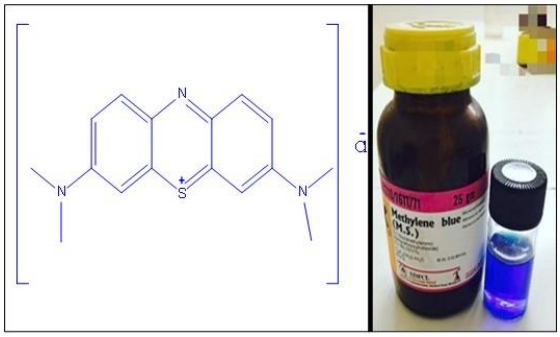

Fig 3. Methylene Blue

Methylene blue dye was taken whose standard absorbance lies in visible region of 675. Firstly, 0.01 mM dye was prepared. From the prepared dye solution, 5 ml of it was added to a test tube and 15 mg of the catalyst was added. It was placed in sunlight with continued magnetic stirring for the suitable time for which the dye degraded. Every time it's UV was recorded.

Photoreduction of nitro compound

Nitrobenzene is an aromatic nitro compound with chemical formula $C_6H_5NO_2$ and molecular weight of 123.111g/mol. Primarly it is used for production of aniline, but also have some applications in manufacture of pesticides, dyes, drugs, lubricating oils, and synthetic rubber. It is highly toxic and causes severe damage to humans systems. It is soluble in organic solvents like: ethanol, diethyl ether, acetone, benzene but insoluble in water.

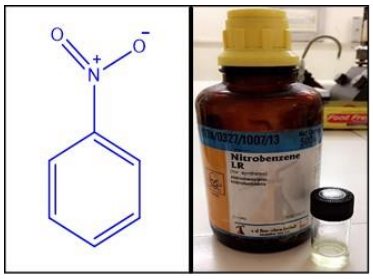

Fig 4. Nitrobenzene

In a test tube, 25µmol solution of nitrobenzene, 5 ml of isopropyl alcohol and 15 mg of the catalyst were added. Argon purging was done for 10 min for each catalyst in the test tube. After purging with Argon, test tubes were covered. The test tubes were placed in sunlight for 6-7 hours so that reduction takes place. The retention time was measured using HPLC.

Characterization techniques

UV- Visible spectroscopy

Photodegradation of dye spectrum was observed with the aid of UV-Visible spectrophotometer. It is related to absorption spectroscopy in the ultraviolet-visible spectral region and uses light near UV and near IR regions. Molecules containing non-bonding electrons can absorb energy in the form of visible light or ultraviolet to excite the electrons to higher molecular orbital's [47]. The easily the electrons excite, the longer is the wavelength of light it can absorb.
The method is based upon the Beer-Lambert law:

$$\mathbf{A=\log_{10}(I_0/I) = €cl}$$

This law holds good for dilute solution only.

Diffused reflectance spectrometer (DRS)

DRS is used to determine absorbtion of MnO_2 nanomaterials. Using Avantes Diffuse Reflectance Spectrometer the analysis was done. 2-5 mg of sample was taken on glass-slide and placed the light source over it to record absorption spectra by taking $BaSO_4$ as reference. By using Beer-Lambert law, it can be used for quantitative photometric analysis.

X-Ray Diffraction

Using X-ray diffractometer, crystalline properties of sample were characterized by CuKα-radiation source at λ=1.54Ă at 20mA current and 30 kV voltage. X-Ray diffraction follows Brag's Law, here Brag's angle ranges from 20 to 70 and crystallite size was calculated using scherrer's equation d= kλ/ßCosθ, where λ is wavelength, θ is diffraction angle, d is crystallite size, k is constant, ß is full width at half maxima of diffraction line. MnO_2 samples were analyzed at SAI LABS Thapar University.

Scanning Electron Microscopy (SEM)

SEM is used for the study of external morphology and relative amount of as prepared constituents as atom % = weight % or atom % = Wt. %. The MnO_2 samples were analyzed using JSM-7600F at SAI LABS Thapar University.

Fluorescence spectroscopy

Photoluminescence (PL) spectroscopy indicates presence of surface defects. In agreement with earlier results, lower the intensity of band, more is the quenching.

Dynamic Light Scattering (DLS)

DLS is used for determining the particle size of MnO_2 nanoparticles. In DLS the measurements are dependent on size of particles and surface charge attained by particles at different concentrations. Due to brownian motion of particles, DLS spectra is observed. This measures variations in intensity of scattering light. DLS mainly tells us about the particle population and diameter. Here, MnO_2 nanoparticles are taken in cuvvete and dispersed in water through sonication.

High Performance Liquid Chromatography

Separation and detection of amino compound was performed using HPLC instrument consisting of auto sampler and water pump. The experiment was performed at 28°C and a UV-detector was applied at 295nm. Reverse phase column was used. Solvent mixture of water and methanol with ratio 70:30 (v/v) at flow rate of 1mL min^{-1} and injection volume was 20 mL with injection volume of 20 μL [49]. The principle involves separation of two different substances on the basis of their migration rates. As it follows reverse phase so more the material is non polar, more it is retained in it. Hence amines have more polarity as compared to nitro compounds, so they elute first.

Gas Chromatography

GC (GC (Nucon 13A Porapak-Q column with TCD detector)) is used to quantify the amount of CO_2 produced during dye degradation. The GC-oven temperature was set at50°C injector and detector temperatures were set at 80°C and 90°C respectively. The quantification of CO_2 was done against a standard (180 ppm) with retention time of approximately 0.57 min.

Results and discussion

The composition of the samples and content of manganese nanoparticles were characterized with the help of different techniques and the respective results are as under:

Diffused reflectance spectrometer (DRS)

The UV–Vis absorption spectra of all MnO_2 photocatalysts are presented in Fig 5. , which shows a typical absorption edge in between 350 and 650nm. Some red shift is observed in gama nanosheets and nanospheres which causes shift of absorption frequency.

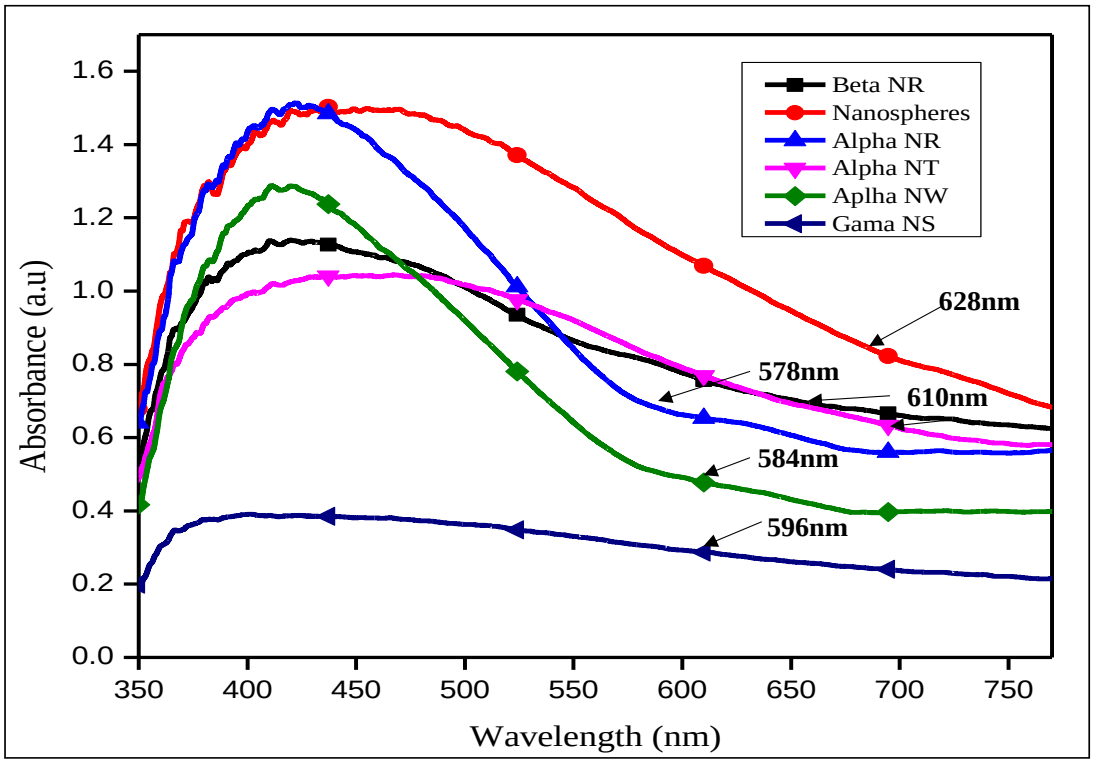

Fig 5. Diffuse Reflectance Spectra of various morphologies of MnO_2

X-Ray Diffraction

Fig 6. represents XRD patterns of hydrothermally synthesized MnO_2 nanomaterials. In these XRD patterns, the reflections of alpha nanotubes, alpha nanowires and alpha nanorod scan be depicted as body-centered tetragonal α-MnO_2 (JCPDS no. 44-0141, space group 14/m, a = b = 9.784 Å, c = 2.863 Å), indexing towards the significant phase-purity of the acquired α-MnO_2 materials. As seen from Fig 6. alpha nanotubes have maximum peak at plane (211) at 2θ = 37° and other planes are (220), (521), (510), (600), (002) while alpha nanowires have similar maxima at 2θ =37° and other plane at (002). In case of alpha nanorods the maxima is achieved at 2θ = 36.4° where other peaks corresponds to planes (211), (300), (002).ß-MnO_2 nanorods (JCPDS 24-0735) can be depicted as tetragonal phase. Plane (101) is present in all nanomaterials at 2θ = 37°.The lattice constants were calculated, and a is 4.38 Å and c is 2.88 Å, which are very consistent. The intensity of (101) is highest which represents the preferential growth of nanomaterial. Gama nanosheets (JCPDS 30-0820), could be identified as hexagonal MnO_2. It can be easily listed to the lattice constants (a = 2.80 °A, b = 2.80 °A, c = 4.45°A. A closer look into the (110) peaks of MnO_2 depicts considerable high-2θ = 31°. Nanospheres have maximum peak at plane (211) at 2θ = 36.1° while other peaks at (103), (411), (521), (002) and (541).

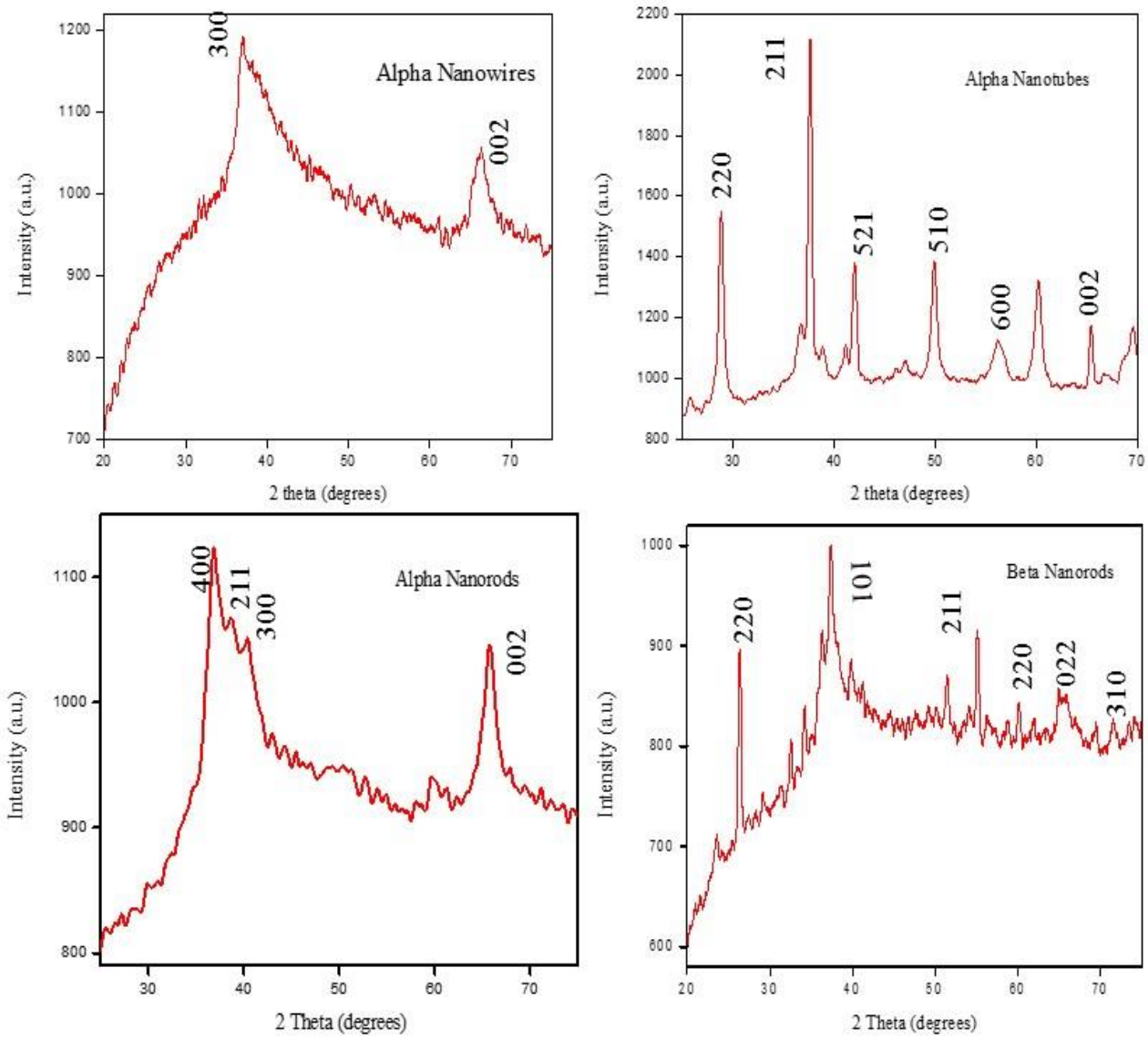

Fig 6. XRD spectra of various shapes of MnO_2

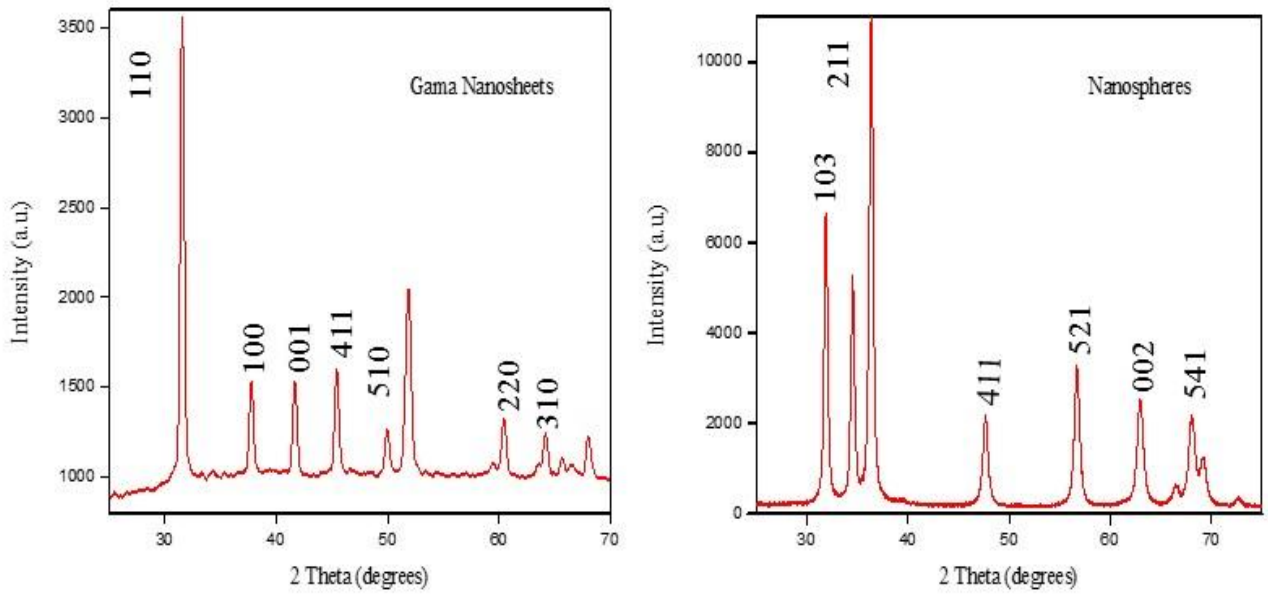

Fig 6. XRD spectra of various shapes of MnO_2

Table 3: Comparative study of XRD spectra of various morphologies of MnO_2

S. No	Photocatalyst	XRD peaks	Crystal structure
1.	Alpha nanorod	(400), (211), (300), (002)	Body centered Tetragonal
2.	Beta nanorod	(220), (101), (211), (220), (002)	Tetragonal phase
3.	Alpha nanowire	(211), (002)	Body centered Tetragonal
4.	Alpha nanotube	(211), (220), (521), (510), (002),(6000	Body centered Tetragonal
5.	Nanospheres	(211), (103), (411), (521), (002), (541)	Tetragonal
6.	Gama nanosheets	(110), (1000, (001), (411), (510), (220), (310)	Hexagonal phase

Scanning Electron Microscopy

The SEM images of various synthesized MnO_2 morphologies have been shown in Fig 7.1 (a), where alpha nanotubes are shown to have smooth flower like shape and these are appearing to come outwards. A large number of alpha nanotubes are presented in Fig 7.2 (b). MnO_2 alpha nanorods are presented in Fig 7.2 (c), which are uniformly placed with approximate diameter of 1μm. These high-purity MnO_2 nanorods are about 2.85μm in diameter. Fig 7.3 (e, f) shows gama nanosheets of approximate diameter of 2μm and are uniformly distributed while nanospheres in Fig 7.3 (g) are of approximate diameter of 5 μm and these are aggregated together. A large number of beta MnO_2 nanorods are presented in Fig. 7.4 (i, j), where the nanorods are shown to have typical rod-like shape in agglomerated form. The nanowire Fig 7.4 (k) morphology grown into few micrometer length wire with a ~1.78μm diameter. EDX spectra shown along with SEM images represents elementary composition.

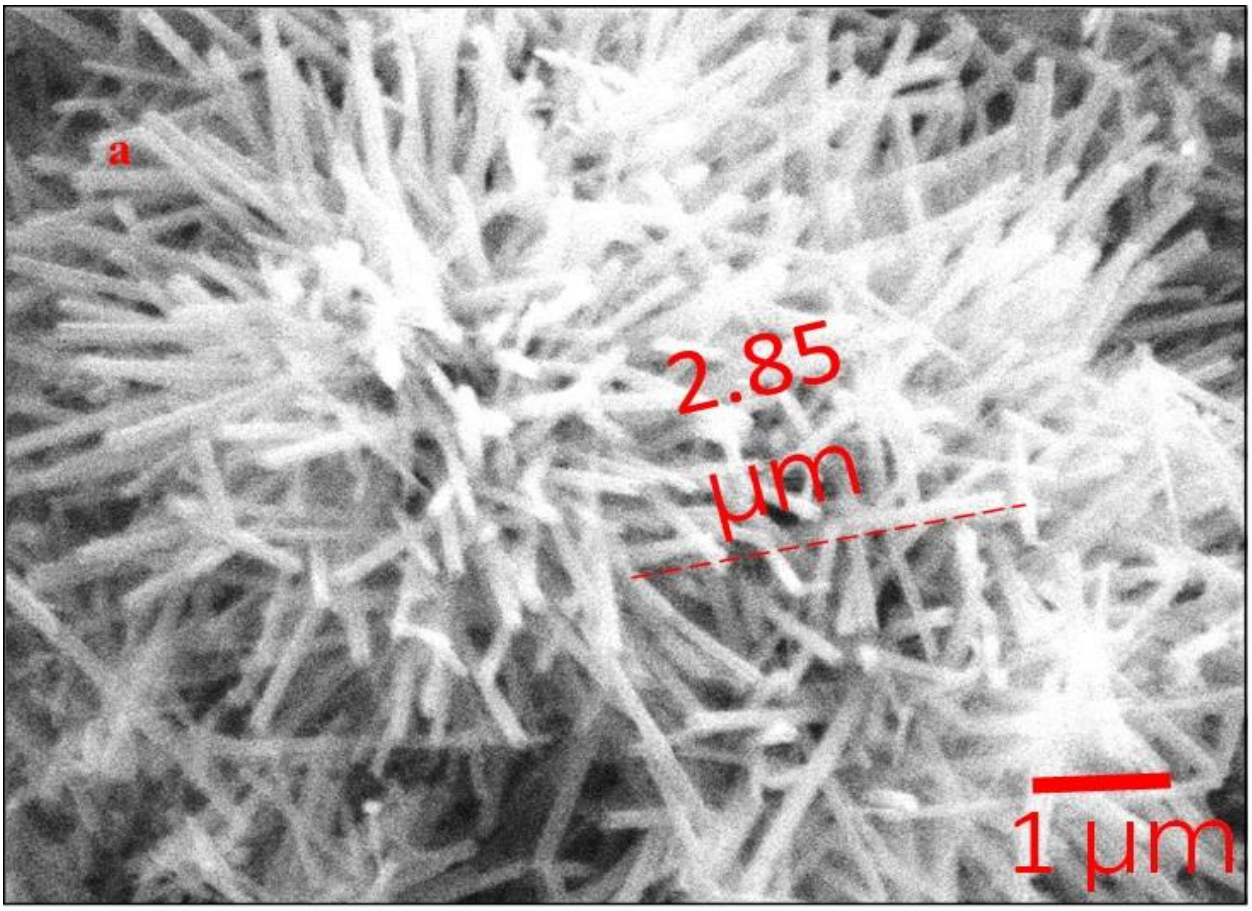

Fig 7.1 (a) SEM image of Alpha Nanotube of MnO_2

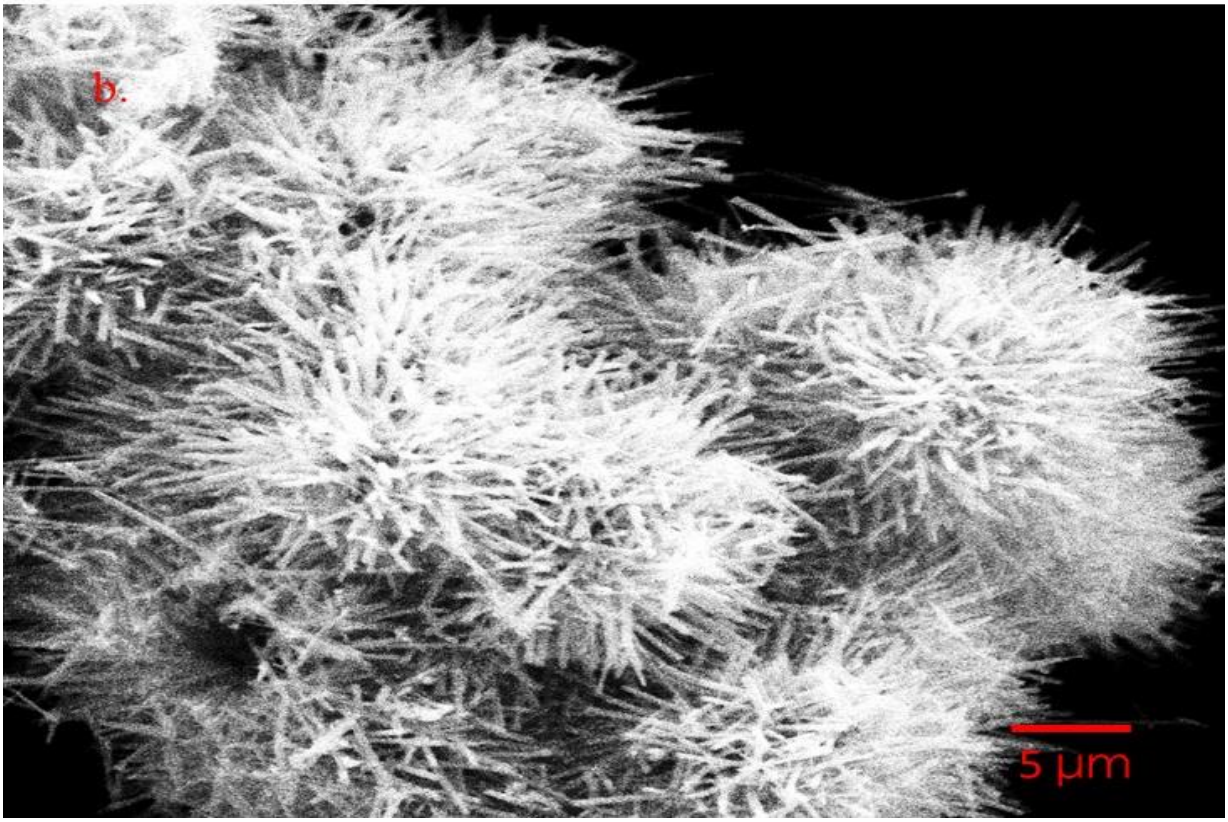

Fig 7.2 SEM image (b) Alpha Nanotube of MnO_2

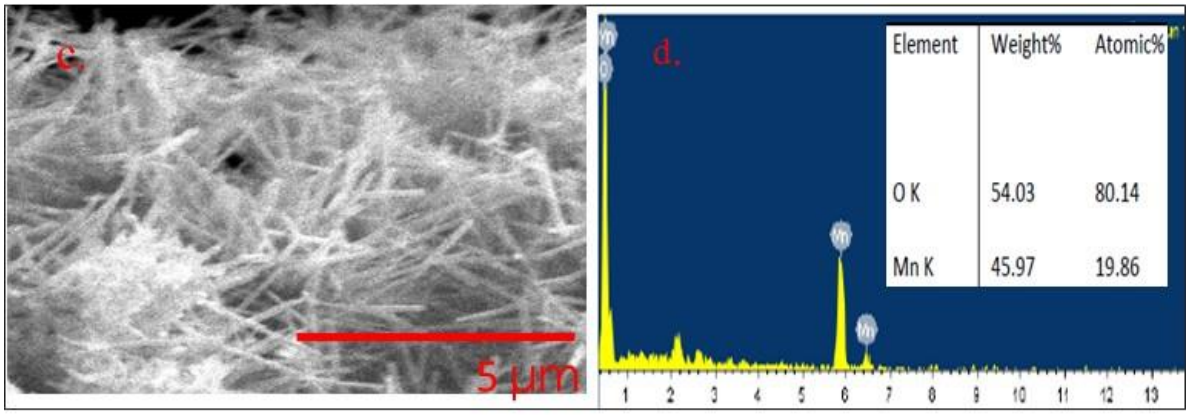

Fig 7.2 SEM image of (c) Alpha Nanorods (d) EDS spectra of MnO_2

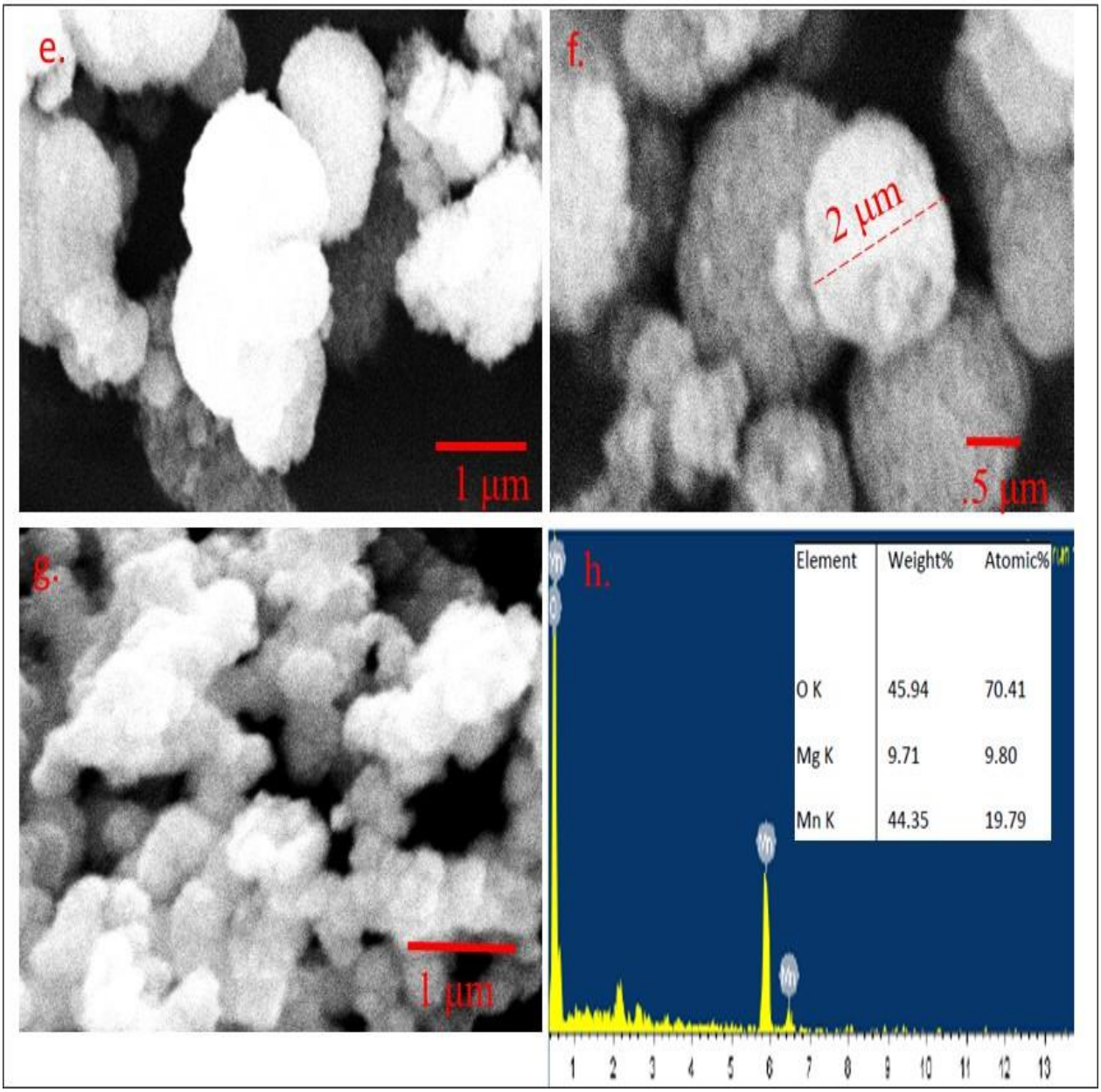

Fig 7.3 SEM images of (e, f) Gama Nanosheets, (g) Nanospheres, (h) EDX spectra of MnO_2

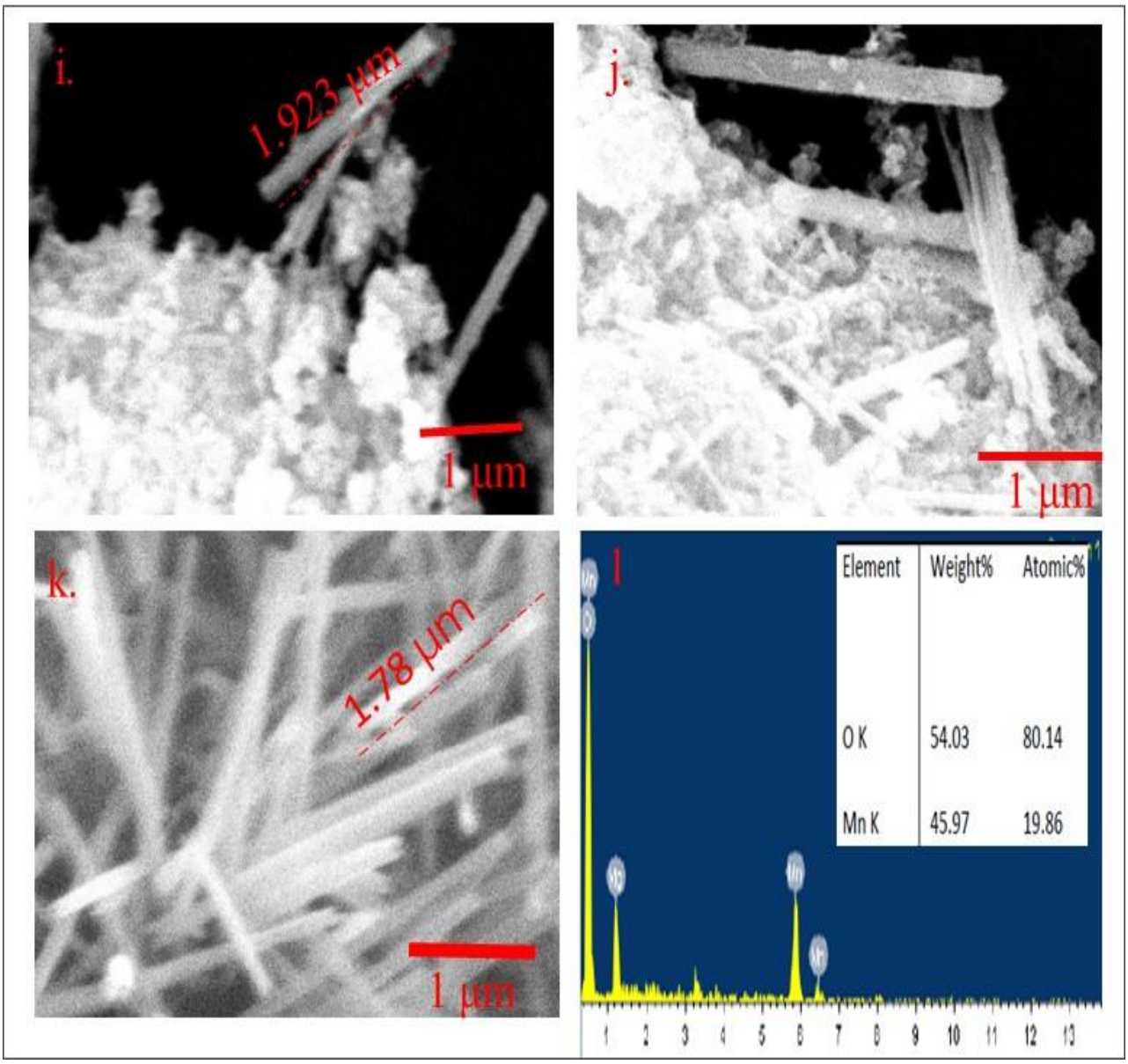

Fig 7.4 SEM images of (i, j) Beta Nanorods, (k) Alpha Nanowires, (l) EDX spectra of MnO_2

Fluorescence spectroscopy

Comparatively, Beta nanorods and alpha nanotubes have low intensity and more quenching because of presence of trap sites present on the surface. Photoluminescence quenching can be viewed because of effective distribution of electrons along larger interfaces from CB which enables the separation of charge carriers and prevents the recombination of electrons and holes. From Fig 8. more quenching is observed in case of beta nanorods due to its dimensionality which helps in redistribution of electrons along larger interface leads to enhancing of its lifetime.

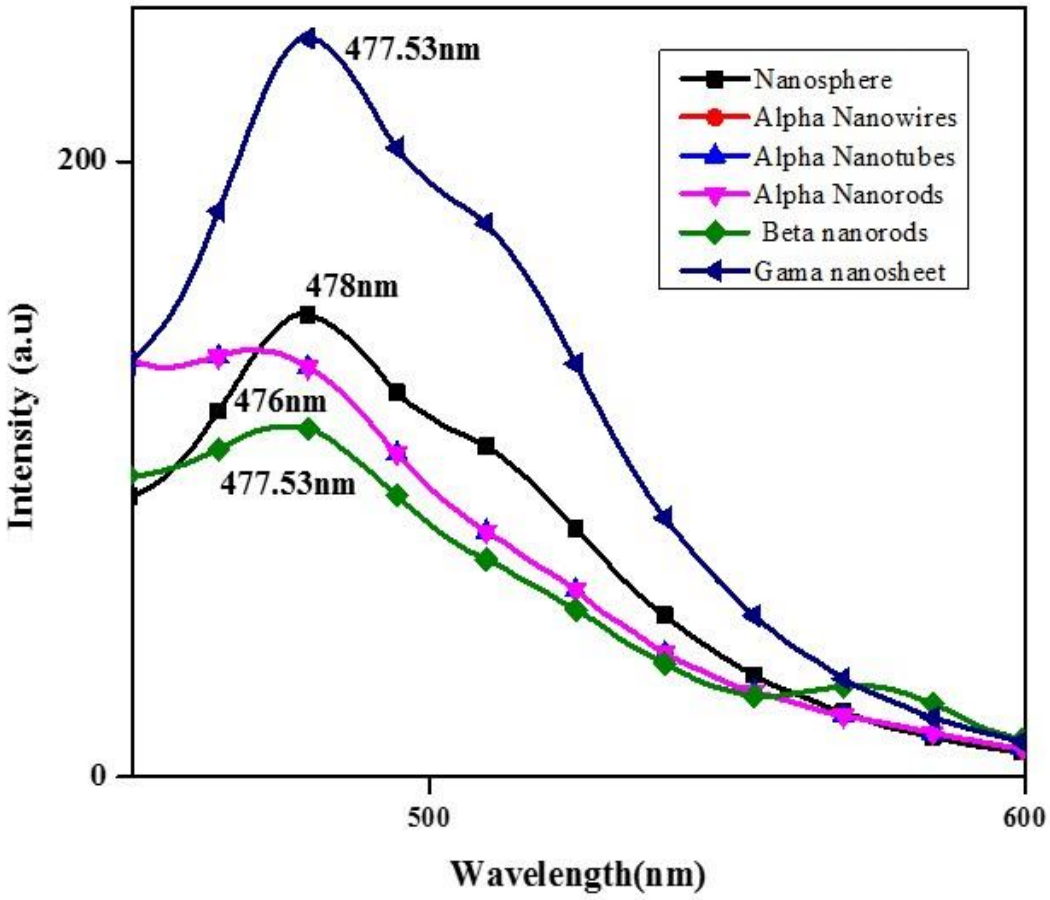

Fig 8. Photoluminescence spectra of different photocatalysts of MnO_2

Dynamic Light Scattering (DLS)

Here, MnO_2 nanoparticles are taken in cuvvete and dispersed in water through sonication. DLS shows size range of alpha nanorods, gama nanosheets, alpha nanotube, beta nanorods is 50nm, 95 nm, 90-190nm, 89-260nm respectively. The range of alpha nanowires and nanospheres is 1331nm and 772nm respectively. Fig 9. shows DLS spectra of various MnO_2.

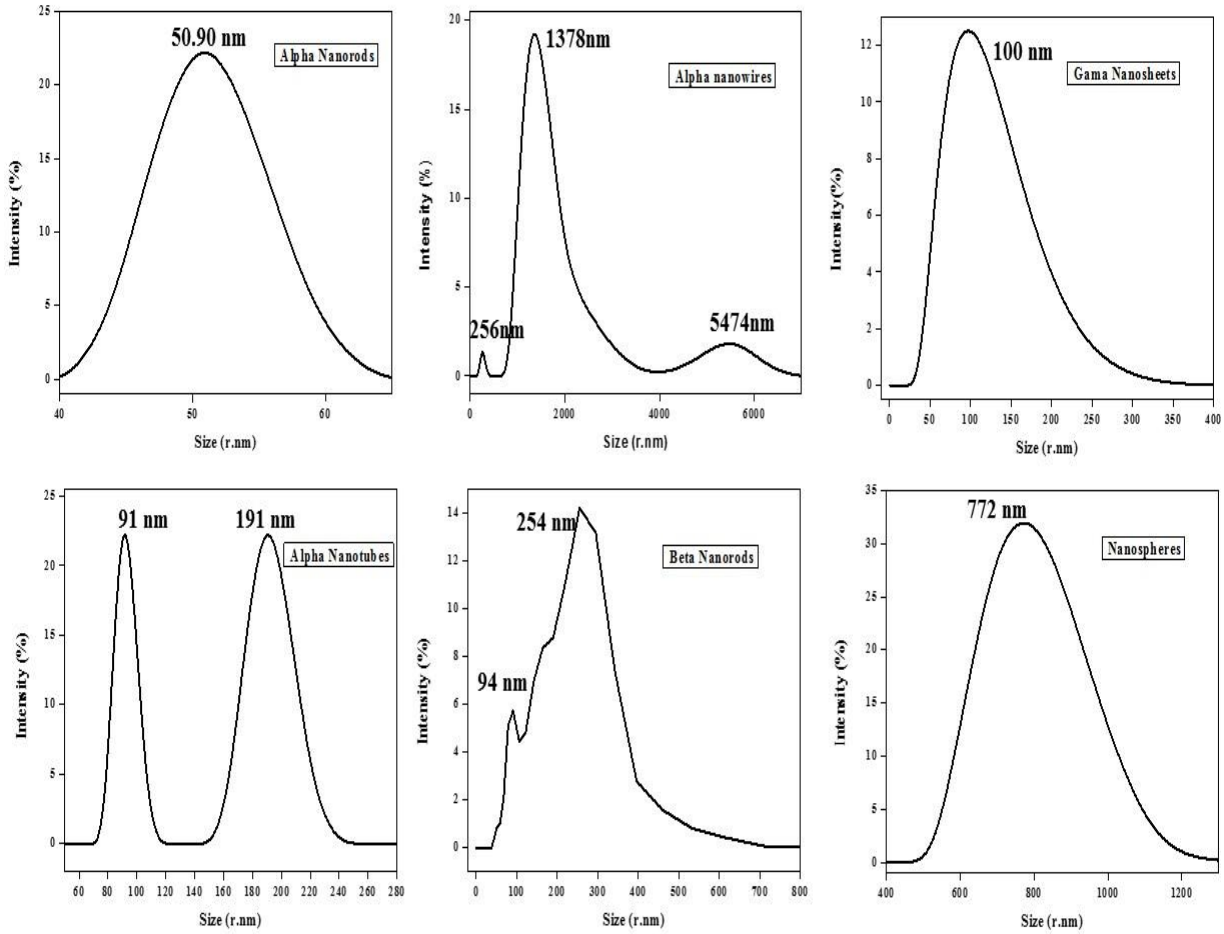

Fig 9. Dynamic Light Scattering of various shapes of MnO_2

Photocatalytic activity of prepared catalyst

A. Photo oxidation of methylene blue dye

The photocatalytic activity of photocatalyst MnO_2 was observed by using methylene blue dye. The whole experiment was done under sunlight irradiation for different time intervals. Here, methylene blue dye solution (5ml) with MnO_2 photocatalyst (15 mg) was irradiated for various time intervals and photocatalytic activity was observed. The absorption peak near 600-700 is due to absorption of conjugated system whereas peak near 300 is due to aromatic ring absorpton. Observed earlier that π-$\pi*$ and n– $\pi*$based chromophore breaks first because of dissociation of aromatic ring. MnO_2 catalyst depicts higher levels of photocatalytic degradation. In all the six

MnO_2 photocatalysts intensity of absorption band of MB decreases gradually with time course because of mineralization

n of MB dye under longer sunlight light irradiation [48]. From the slope of change in concentration, the rate constant can be calculated and was observed to follow the pseudo first order kinetics as per following equation.

$$\mathbf{Ln}\ C / C_0 = -\mathbf{k}\ \mathbf{t}$$

Where, k = Pseudo first order rate constant (min−1), C = Concentration after time t and C_0 = Initial concentration Using, $\boldsymbol{k = 2.303 \times slope}$ it can be calculated.

The color of MB suspension vanishes within 3 hours in case of gama nanosheets, alpha nanowires, beta nanorods (Fig 10.) and in 8 hours in case of alpha nanorods alpha nanotubes (Fig 10.) and nanospheres. Fig 11. , Fig 12. indicating its degradation to smaller intermediates whereas, increase in CO_2 level was observed up to 4 hours, indicating complete photomineralization of MB. Fig 13. represents the photodegradation efficiency of various catalysts and shows efficiency of beta nanorods and alpha nanors is highest as compared to other catalysts.

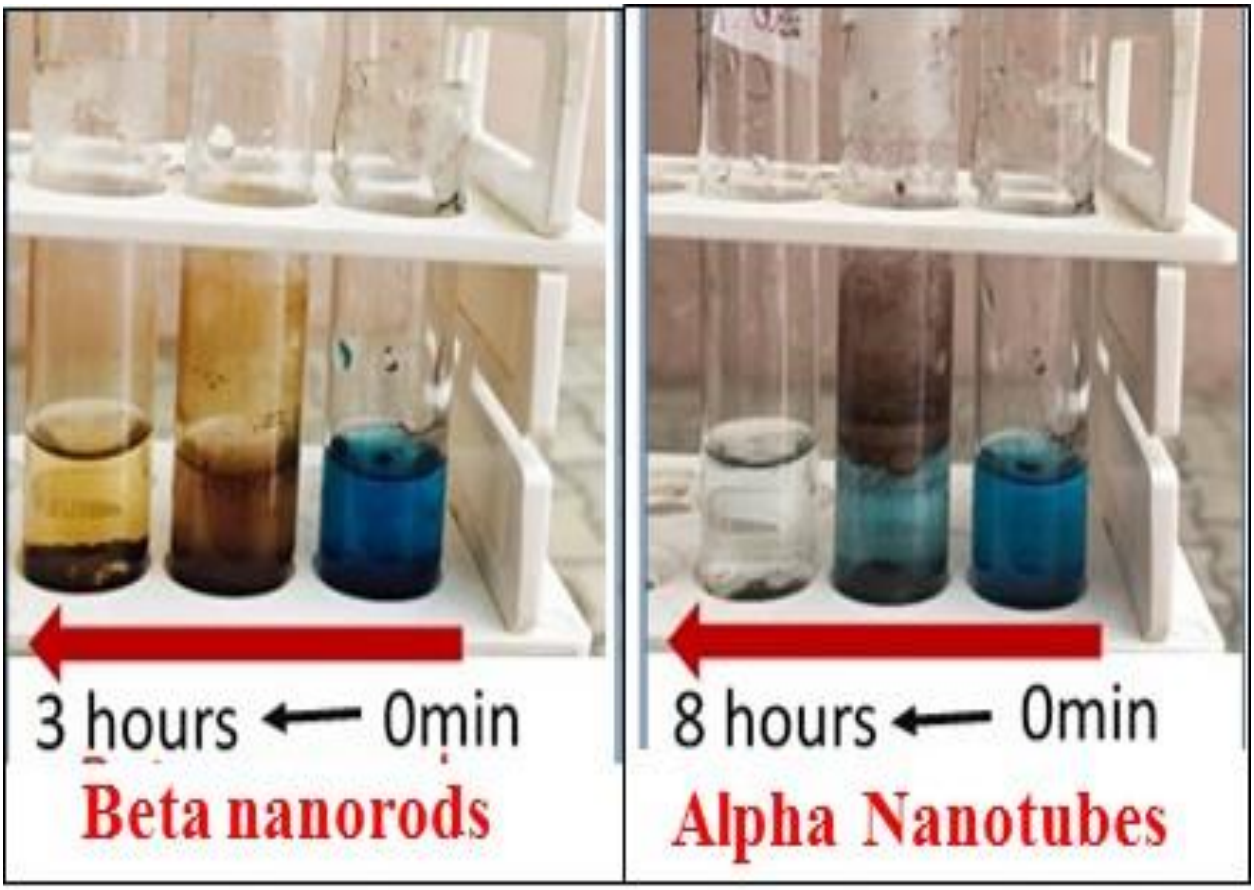

Fig 10. Degradation of Methylene Blue with beta nanorods and alpha nanotubes of MnO_2

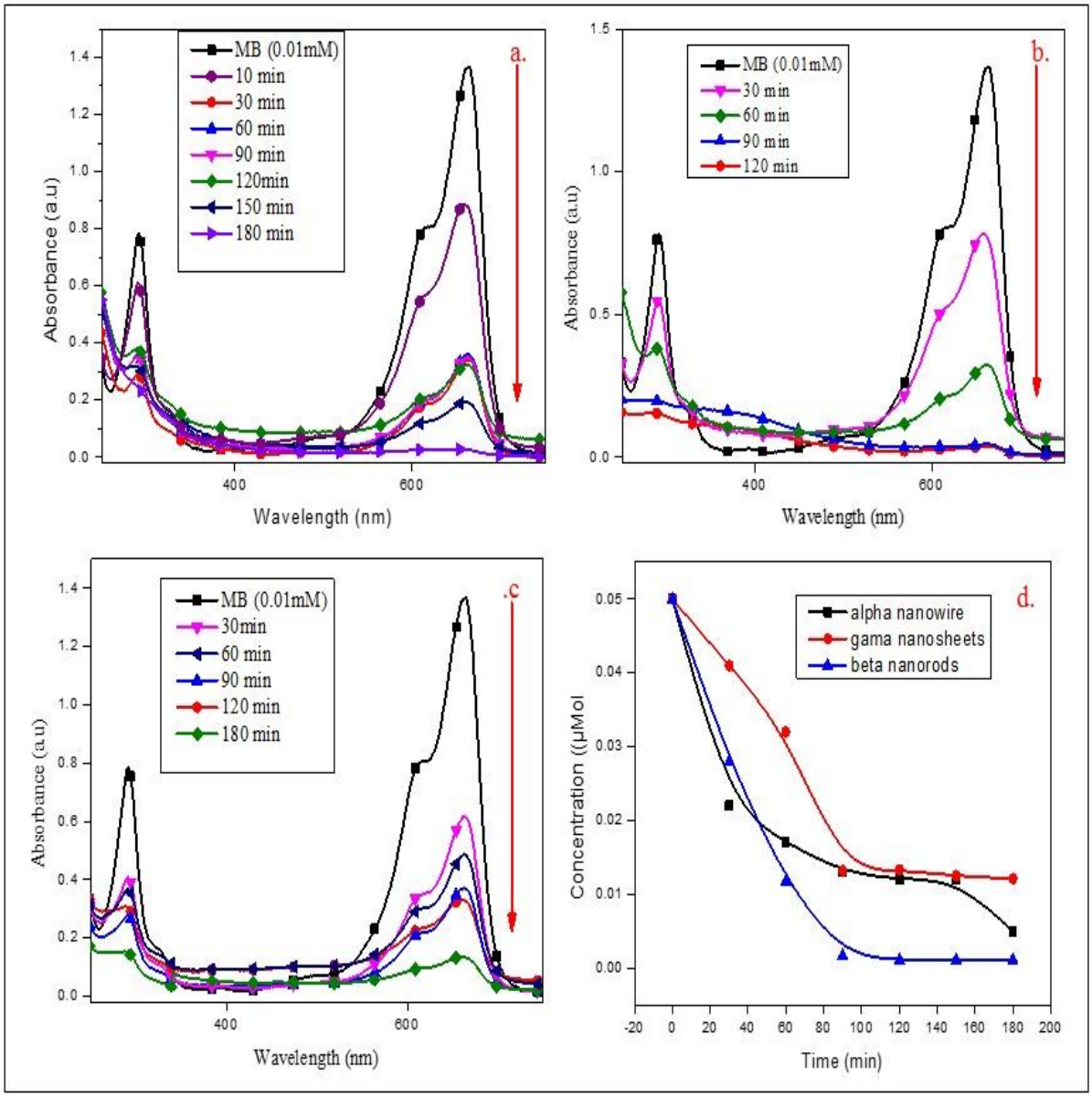

Fig 11. Photocatalytic degradation of Methylene Blue using different morphologies of MnO_2 (a) Beta Nanorods, (b) Gama Nanosheets, (c) Alpha Nanowires and (d) Time vs Concentration

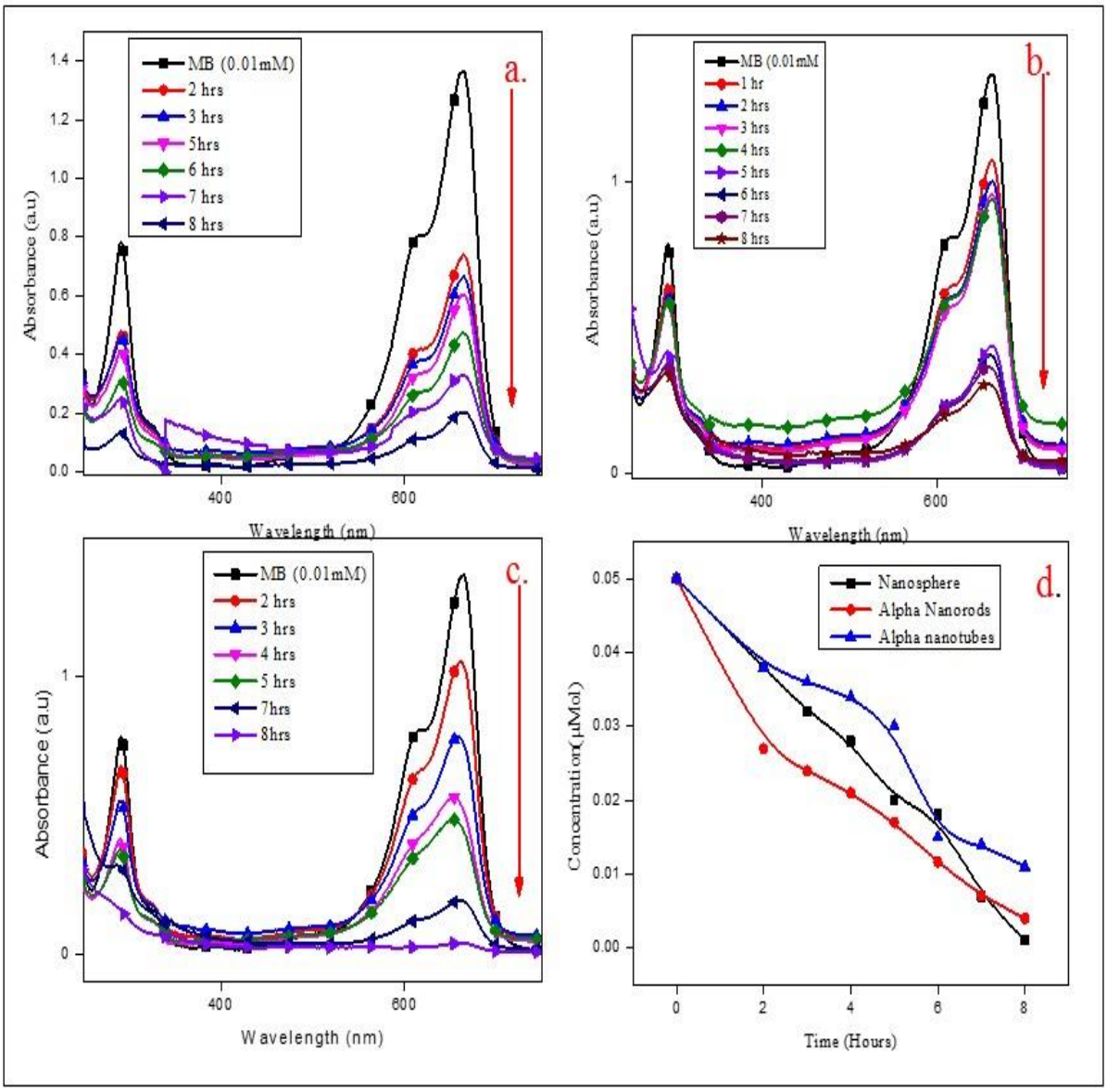

Fig 12. Photocatalytic degradation of Methylene Blue using different morphologies of MnO_2 (a) Alpha Nanorods, (b) Nanospheres, (c) Alpha Nanotubes and (d) Time vs Conc.

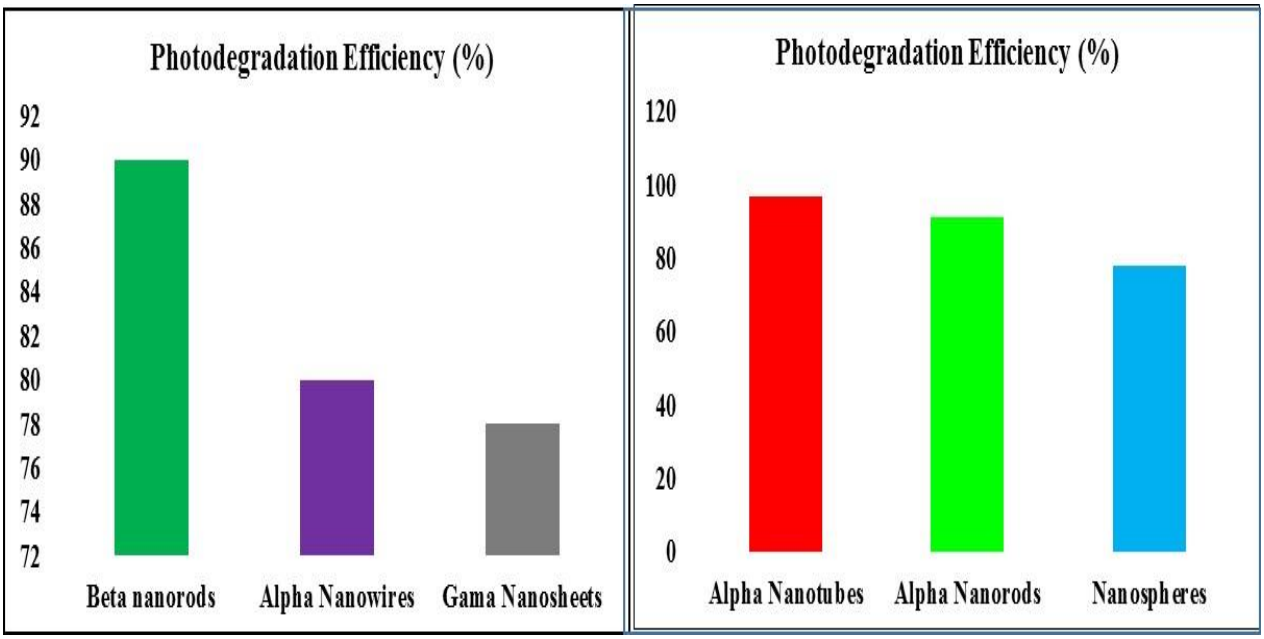

Fig 13. Photodegradation efficiency of Methylene Blue with various MnO_2 photocatalysts

Quantification of CO_2 by GC

As dye degrades to produce CO_2 and H_2O. The evolution of CO_2 during photodegradation of methylene blue was analyzed by GC as shown in Fig 15. It shows that alpha nanotubes and beta nanorods have highest photocatalytic activity.

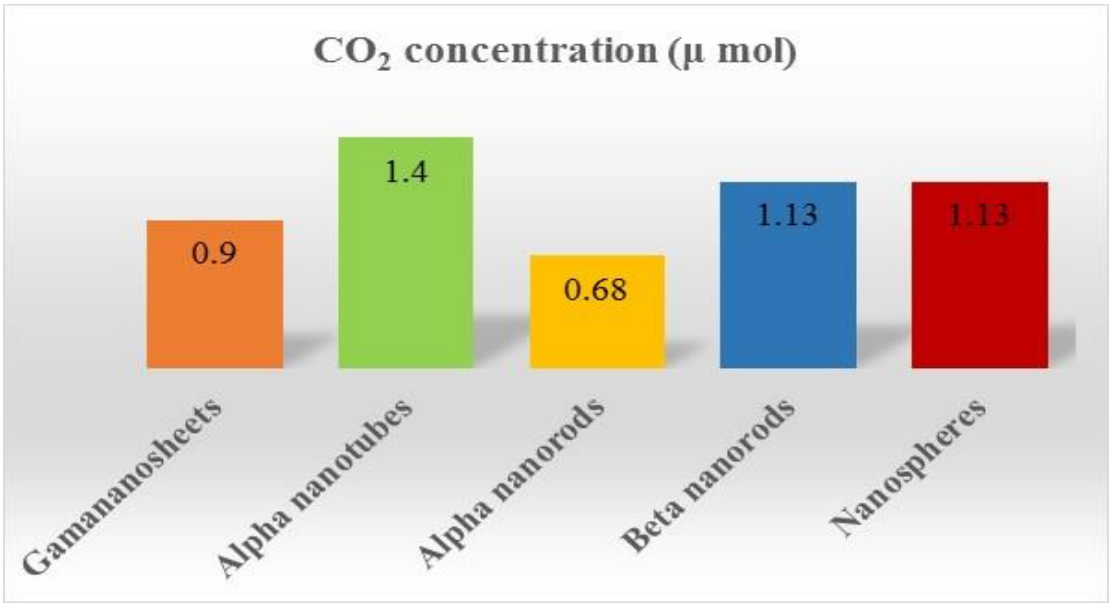

Fig 14. CO_2 evolution by photo oxidation of methylene blue

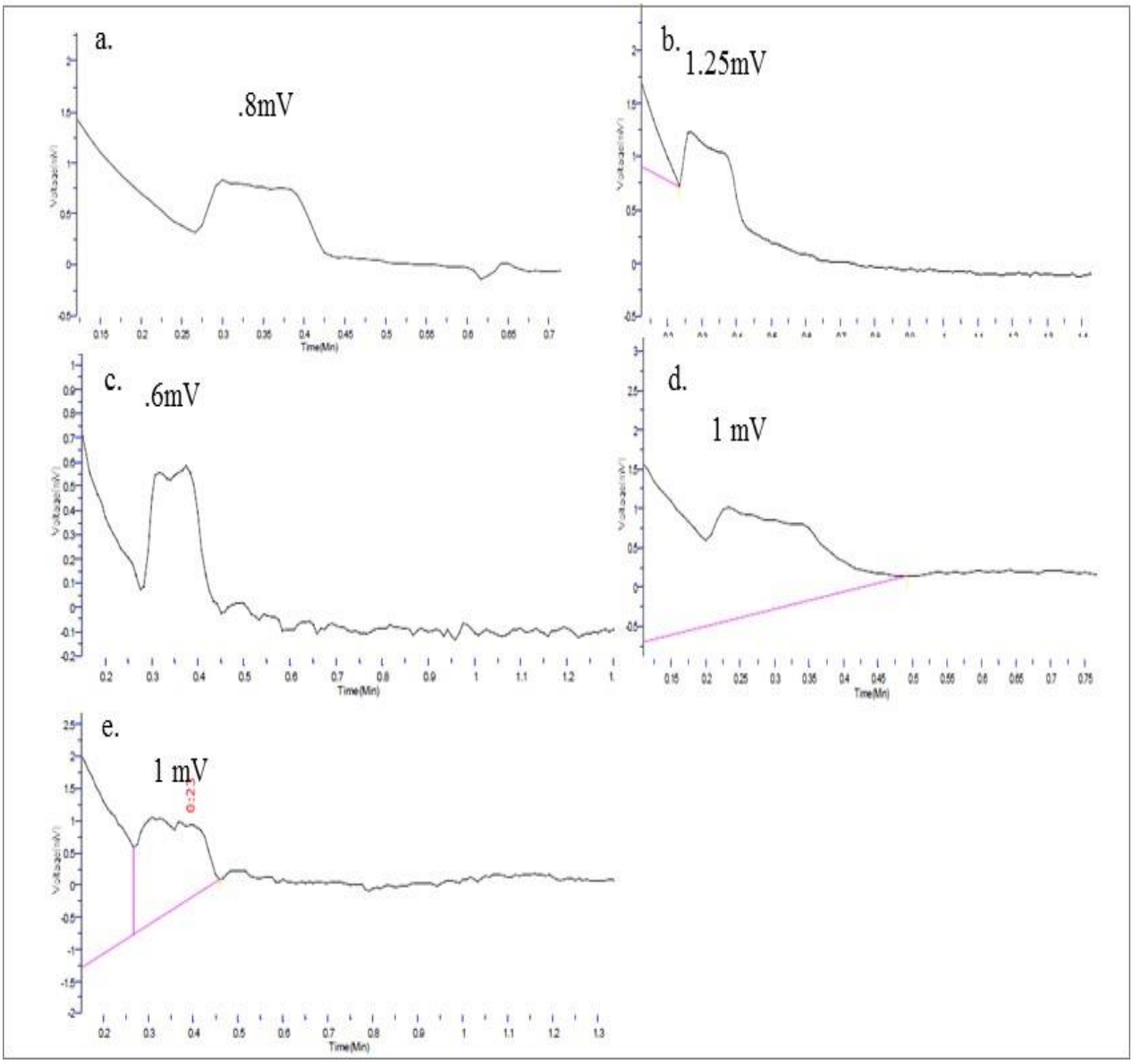

Fig 15. GC spectrum for CO_2 evolution with various MnO_2 photocatalysts (a) Gama Nanosheets, (b) Nanospheres, (c)Alpha Nanorods, (d) Alpha Nanorods, (e) Alpha Nanotube

B. Photoreduction of nitrobenzene

It is another application including conversion of toxic nitrobenzene to aniline using photocatalyst MnO_2. Here, isopropyl alcohol was taken as solvent as it has better hole scavenging capacity [49] than other primary alcohols and also shows better electron giving ability for reduction process. In this experiment, 15 mg of photocatalyst was added to 5ml of isopropyl alcohol containing nitrobenzene (25μmol). The results were analyzed by HPLC. A comparative HPLC

pattern shows a clear separation of nitrobenzene (t_R = 4.8 min), aniline (t_R = 3.6 min) peaks in a mixture (5 mM) of authentic samples, and nitrobenzene reduction by MnO_2 for 8 h irradiation displayed aniline formation at t_R = 3.6 min.

Fig 16. , Fig 17. showed that nitrobenzene (25 µmol) is selectively reduced to 80% aniline (20.5 µmol) by alpha nanotubes of MnO_2 catalyst and other catalysts are reduced to 1-20% of aniline. Also it showed that 82.2% of nitrobenzene is converted into aniline as shown in Fig 18.

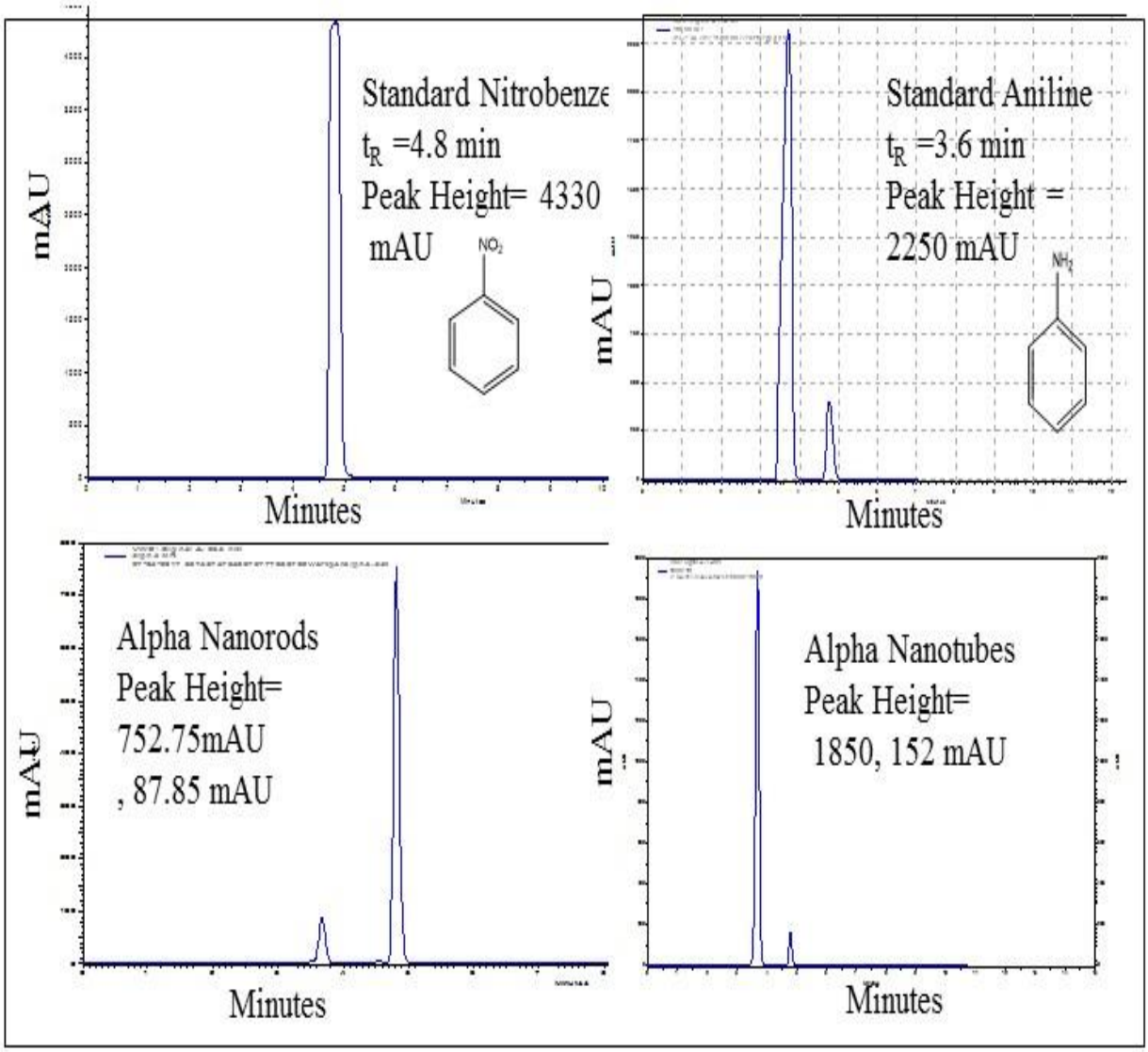

Fig 16. Time course of standard nitrobenzene and aniline and photoreduction of Nitrobenzene (25 µ mol) by different MnO_2 photocatalyst in Isopropyl Alcohol under 8 h solar irradiation

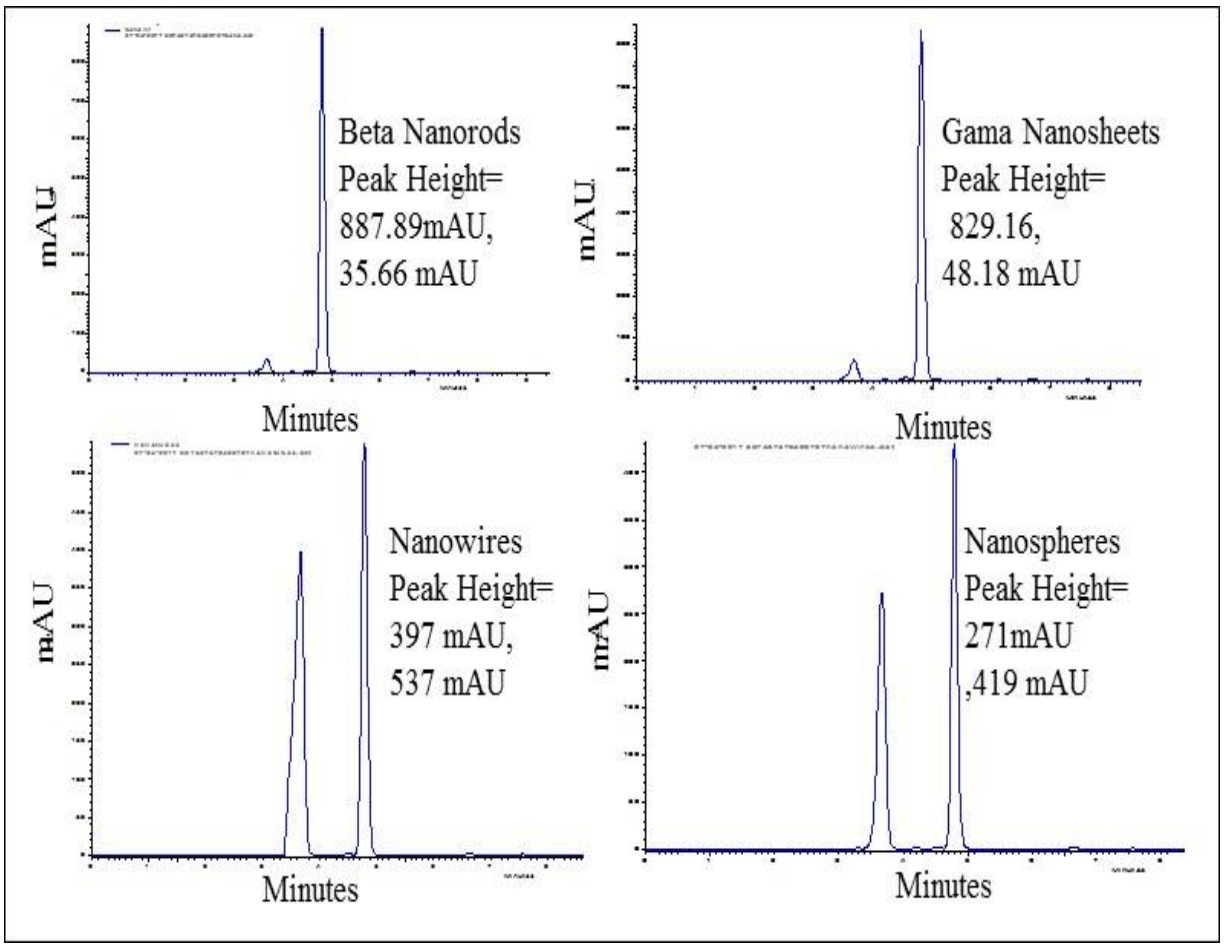

Fig 17. Time course of photoreduction of Nitrobenzene (25 µ mol) by different MnO_2 photocatalystin Isopropyl Alcohol under 8 h solar irradiation.

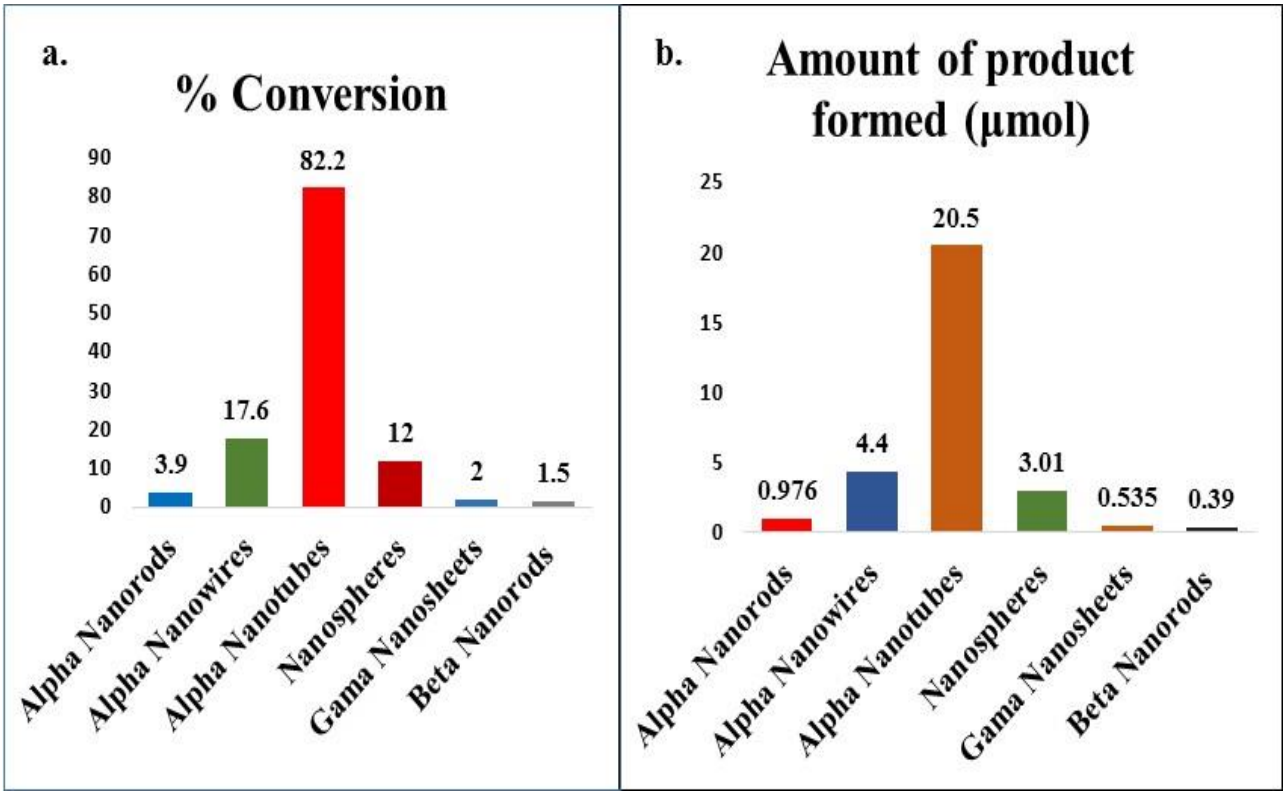

Fig 18. (a) % reduction of Nitrobenzene to aniline by MnO_2 for 4 h (b) amount of product formed in iso-propanol after 8 hours solar irradiation.

Reaction mechanisms

A. Mechanism of Photo oxidation of Methylene blue

On the basis of the previous discussions, the photocatalytic degradation of Methylene Blue is seemingly as through various steps. The first step of photo catalysis is generation of electron-hole pair in MnO_2 under solar light. After absorption of energy equal to or greater than the band gap of MnO_2 holes are generated in valence band and electrons in conduction band. Photoelectrons reduce O_2 to oxygen radicles ($\cdot O_2^-$) and then to hydroxyl ($\cdot OH$) Radicles. Further holes oxidize H_2O to hydroxyl radicals. These hydroxyl have ability to oxidize methylene blue and decompose it into further intermediates these intermediates are highly unstable in presence of $\cdot OH$ radical and gets converted to aliphatic acids that finally break down to produce carbon dioxide (CO_2) and water (H_2O) (Scheme 4)

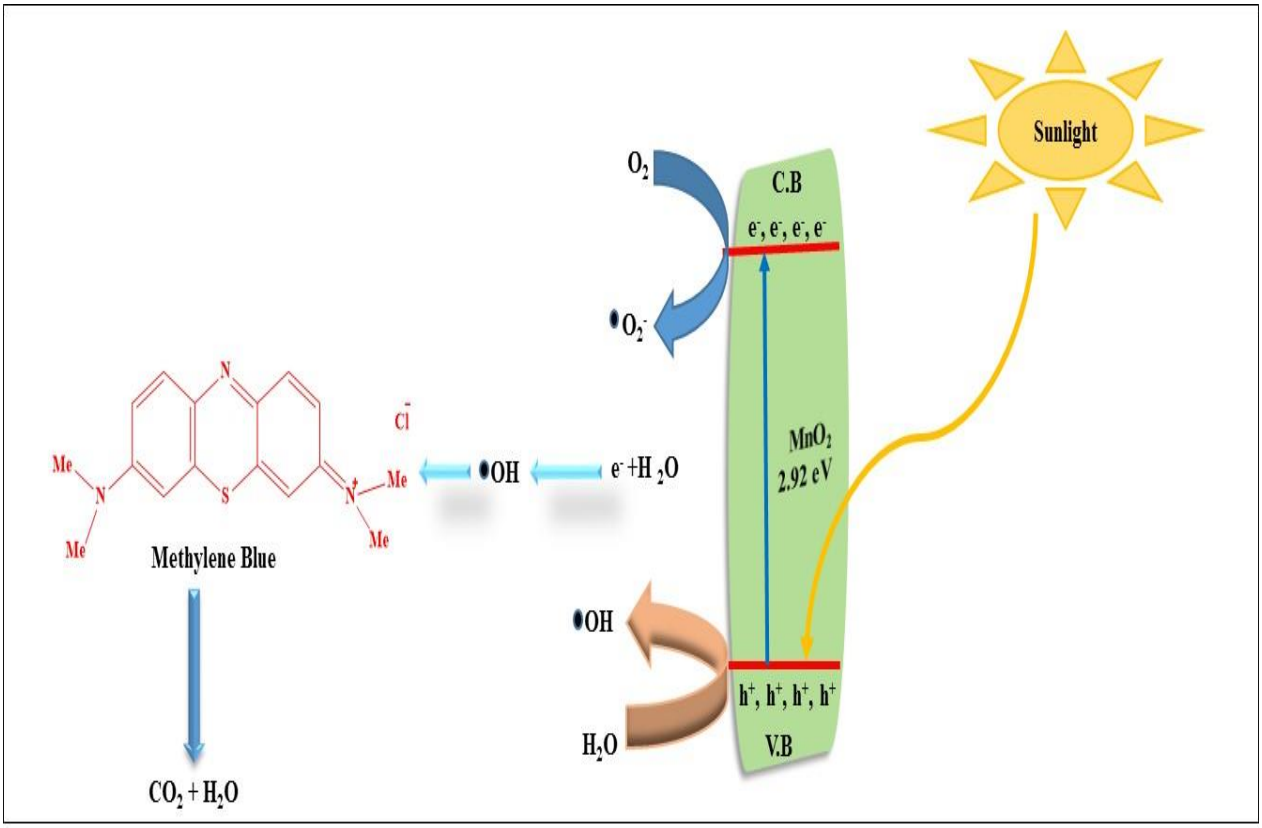

Scheme 4: Complete degradation of Methylene Blue with MnO_2 photocatalyst under sunlight

B. Mechanism of Photoreduction of Nitrobenzene

The photocatalytic reduction of nitrobenzene is shown in scheme 5. First step of photo catalysis is generation of electron-hole pair in MnO_2 under solar light. After absorption of energy equal to or greater than the band gap of MnO_2 holes are generated in valence band and electrons in conduction band. Thus, the two processes that occur in series, one is generation and migration of generated photoelectrons and holes and the other is reaction between these electron-hole pairs or hydroxyl radical and organic compound. Therefore, for the overall process, each step can be rate-determining step. In valence band isopropyl alcohol is converted to acetone and photoelectrons in conduction band reduce nitrobenzene to aniline.

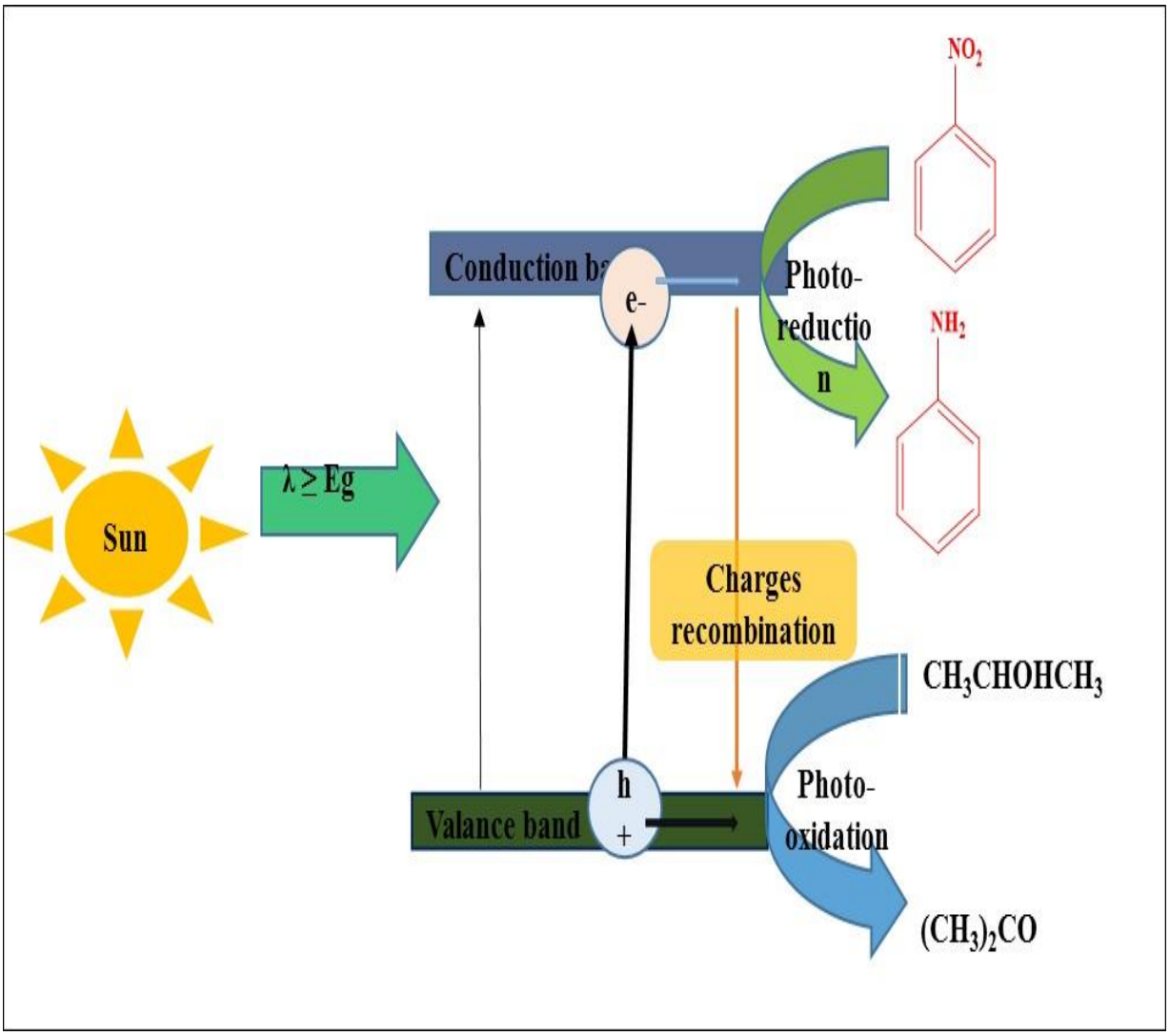

Scheme 5: Complete reduction of Nitrobenzene with MnO_2 photocatalyst under sunlight

7. Conclusion

The work demonstrated the preparation of varying morphologies of MnO_2 for enhancing the photocatalytic activity. Alpha MnO_2 nanotubes and Beta MnO_2 nanorods are effective photocatalysts for photo oxidation of methylene blue resulting in complete photo mineralization to H_2O and CO_2. This work also showed that Alpha nanotubes are effective catalyst for photoreduction of toxic nitrobenzene to aniline under sunlight. Thus it has been concluded that MnO_2 photocatalyst is effective tool for eliminating toxic substances from environment.

References

1. J. C. Colmenares, R. Luque, J. M. Campelo, F. Colmenares, Z. Karpiński, A. A. Romero, Nanostructured photocatalysts and their applications in the photocatalytic transformation of lignocellulosic biomass: an overview, Materials 2 (2009) 2228-2258.

2. A.S. Aricò, P. Bruce, B. Scrosati, J.M. Tarascon, W. Van Schalkwijk, Nanostructured materials for advanced energy conversion and storage devices, Nature materials, 4 (2005) 366-377.

3. I. Chorkendorff, J.W. Niemantsverdriet, Concepts of modern catalysis and kinetics, John Wiley & Sons, 2006.

4. K.J. Laidler, A. Cornish-Bowden, Elizabeth Fulhame, Discovery of catalysis: 100 years before Buchner, Cornish-Bowden, (1997), 123-126.

5. C. Song, Global challenges and strategies for control, conversion and utilization of CO_2 for sustainable development involving energy, catalysis, adsorption and chemical processing, Catalysis today, 115 (2006) 2-32.

6. B. Mitra, D.Vishnudas, S.B. Sant, A. Annamalai, Green-synthesis and characterization of silver nanoparticles by aqueous leaf extracts of Cardiospermum helicacabum leaves, Drug Invention Today, 4(2) (2012) 340-344.

7. M.A. Fox, M.T. Dulay, Heterogeneous photocatalysis, Chemical Reviews, 93, 1993, 341-357.

8. S.M. George, Introduction: heterogeneous catalysis, Chemical Reviews, 95 (1995) 475-476.

9. A.T. Bell, The impact of nanoscience on heterogeneous catalysis, Science, 299 (2003) 1688-1691.

10. A.L. Linsebigler, G. Lu, J.T. Yates, Photo catalysis on TiO_2 surfaces: principles, mechanisms, and selected results, Chemical Reviews, 95 (1995) 735-758.

11. T. Brousse, M. Toupin, D. Belanger, Charge Storage Mechanism of MnO_2 Electrode Used in Aqueous Electrochemical Capacitor, Chemistry of Materials, 16 (2004) 3184–3190.

12. L. Espinal, S.L. Suib, J.F. Rusling, Electrochemical catalysis of styrene epoxidation with films of MnO_2 nanoparticles and H_2O_2, Journal of the American Chemical Society, 126 (2004) 7676-7682.

13. M. Ilyas, M. Siddique, and M. Saeed, Liquid-phase aerobic oxidation of benzyl alcohol catalyzed by mechanochemically synthesized manganese oxide, Chin. Sci. Bull, 58 (2013) 2354.

14. F. Teng, S. Santhanagopalan, D.D. Meng, Microstructure control of MnO_2/CNT hybrids under in-situ hydrothermal conditions. Solid State Sciences, 12, 2010, 1677-1682.

15. N. Greenwood Norman, Earnshaw, Alan. Chemistry of the Elements, Oxford: Pergamon Press, 1984, pp.1218–1220.

16. Preisler, Eberhard, Chemie in unserer Zeit, 14 (1980) 137–48.

17. Q. Feng, H. Kanoh and K. Ooi., J. Mater. Chem., 9 (1999) 319-333.

18. A.R. Armstrong, H. Huang, R. A. Jennings, P. G. Bruce, J. Mater. Chem., 8 (1998) 255.

19. O. Schilling, J. R. Dahn, J. Appl. Cryst, 31 (1998) 396

20. M. Thackeray, M. Prog, Solid State Chem, 25, 1997 pp.1.

21. P.M. De Wolff , J.W. Visser, R. Giovanoli, R. Brutsch, Chimia, 32 (1978) 257.

22. J. Zeng, J.R. Nair, C. Francia, S. Bodoardo, N. Penazzi, Li-O_2 cells based on hierarchically structured porous alpha-MnO_2 catalyst and an imidazolium based ionic liquid electrolyte, Int J Electrochem Sci, 8 (2013) 3912-3927.

23. A. Débart, A.J. Paterson, J. Bao, P.G. Bruce, α-MnO_2 Nanowires: A Catalyst for the O_2 Electrode in Rechargeable Lithium Batteries. Angewandte Chemie, 120 (2008) 4597-4600.

24. Y. Meng, W. Song, H. Huang, Z. Ren, S.Y. Chen, S.L. Suib, Structure–property relationship of bifunctional MnO_2 nanostructures: highly efficient, ultra-stable electrochemical water oxidation and oxygen reduction reaction catalysts identified in alkaline media, Journal of the American Chemical Society, 136 (2014) 11452-11464.

25. M.S. Park, J.H. Kim, K.J. Kim, G. Jeong, Y.J. Kim, Morphological Modification of α-MnO_2 Catalyst for Use in Li/Air Batteries. Journal of nanoscience and nanotechnology, 13 (2013) 3611-3616.

26. N. Mittal, A. Shah, P.B. Punjabi, V.K. Sharma, Photodegradation of rose bengal using MnO_2 (Manganese dioxide), Rasayan J. Chem., 2 (2009) 516-520.
27. J. Ge, J. Qu, Degradation of azo dye acid red B on manganese dioxide in the absence and presence of ultrasonic irradiation, Journal of hazardous materials, 100 (2003) 197-207.
28. S. Li, Z. Ma, L. Wang, J. Liu, Influence of MnO_2 on the photocatalytic activity of P-25 TiO_2 in the degradation of methyl orange, Science in China Series B: Chemistry, 51 (2008) 179-185.
29. S.P. Devipriya, S. Yesodharan, Photocatalytic degradation of phenol in water using TiO_2 and ZnO, 2010.
30. W. Zhang, Z. Yang, X. Wang, Y. Zhang, X. Wen, S. Yang, Large-scale synthesis of β-MnO_2 nanorods and their rapid and efficient catalytic oxidation of methylene blue dye, Catalysis Communications, 7 (2006) 408-412.
31. S. Jana, S. Pande, A.K. Sinha, T. Pal, Synthesis of Superparamagnetic β-MnO_2 Organosol: a Photocatalyst for the Oxidative Phenol Coupling Reaction. Inorganic chemistry, 47, 2008, pp.5558-5560.
32. N.M Najafpour, M. Abasi, M. Hołyńska, Nanolayered manganese oxides as water-oxidizing catalysts: the effects of Cu (II) and Ni (II) ions. RSC Advances, 4 (2014) 36017-36023.
33. M. MahdiáNajafpour, Nano-sized Mn oxides as true catalysts for alcohol oxidation by a mononuclear manganese (II) complex. Dalton Transactions, 44 (2015) 15121-15125.
34. E.A. Jenne (Ed.), Trace Inorganics in Water, ACS Advances in Chemistry Series, Vol. 73, Washington, DC, 1968, 337-387.
35. L.B.Young, H. Harvey, Geochim, Cosmochim Acta, 56 (1992) 1175.
36. N.M. Najafpour, A. Zahraee, E. Amini, M.M. Ahari-Mostafavi, M. Kompany-Zareh, RSC Adv., 4 (2004) 64688-64691.
37. R. Gadde, R. Rao, H.A. Laitinen, Anal. Chem, 46 (1974) 2022-2026.
38. N.M. Najafpour, V. McKee, Catal, Commun, 11, 2010, 1032.
39. N.M. Najafpour , M. Amini, M. Hoły_Nska, M. Zare, E. Amini, New J. Chem. 38 (2014) 5069.

40. L. Espinal, S.L. Suib, and J.F. Rusling, Electrochemical catalysis of styrene epoxidation with films of MnO_2 nanoparticles and H_2O_2. Journal of the American Chemical Society, 126(24) (2004) 7676-7682.

41. Y. Li, Y. Wan, S. Zhan, Q. Guan, Y. Tian, Structure–performance relationships of MnO_2 nano catalyst for the low-temperature SCR removal of NOX under ammonia. RSC Advances, 6 (2016) 54926-54937.

42. X. Wang, Y. Zheng, Z. Xu, X. Wang, and X. Chen, Amorphous MnO_2 supported on carbon nanotubes as a superior catalyst for low temperature NO reduction with NH_3, RSC Advances, 3 (2013) 11539-11542.

43. D.J. Bertino, R.G. Zepp, Effects of solar radiation on manganese oxide reactions with selected organic compounds, Environmental science & technology, 25 (1991) 1267-1273.

44. S. Jana, S. Basu, S. Pande, S.K. Ghosh, T. and Pal, Shape-selective synthesis, magnetic properties, and catalytic activity of single crystalline β-MnO_2 nanoparticles, The Journal of Physical Chemistry C, 111 (2007) 16272-16277.

45. K. Selvakumar, S.M. Senthil Kumar, R. Thangamuthu, K. Ganesan, P. Murugan, P. Rajput, S.N. Jha, D. Bhattacharyya, Physiochemical investigation of shape-designed MnO_2 nanostructures and their influence on oxygen reduction reaction activity in alkaline solution. The Journal of Physical Chemistry C, 119 (2015) 6604-6618.

46. J. Villaseñor, P. Reyes, G. Pecchi, Catalytic and photocatalytic ozonation of phenol on MnO_2 supported catalysts. Catalysis Today, 76 (2002) 121-131.

47. C.B. Ojeda, F.S. Rojas, Process analytical chemistry: applications of ultraviolet/visible spectrometry in environmental analysis: an overview. Applied Spectroscopy Reviews, 44 (2009) 245-265.

48. R.A. Rather, S. Singh, B. Pal, Photocatalytic Degradation of Methylene Blue by Plasmonic Metal-TiO_2 Nanocatalysts under Visible Light Irradiation, Journal of nanoscience and nanotechnology, 16 (2017) 1-7.

49. J. Kaur, B. Pal, 100% selective yield of m-nitroaniline by rutile TiO_2 and m-phenylene diamineby P25-TiO_2 during m-dinitrobenzene photoreduction. Catalysis Communications, 53 (2014) 25-28.

50. H.R. Barai, A.N. Banerjee, N. Hamnabard, S.W. Joo, Synthesis of amorphous manganese oxide nanoparticles–to–crystalline nanorods through a simple wet-chemical technique using K+ ions as a ‘growth director’and their morphology-controlled high performance supercapacitor applications. RSC Advances, 6 (2016) 78887-78908.